

# Emerging Material Technologies for Haptics

Shantonu Biswas and Yon Visell\*

The sense of touch is involved in nearly all human activities, but information technologies for displaying tactile sensory information to the skin are rudimentary when compared to state-of-the-art video and audio displays, or to tactile perceptual capabilities. Realizing tactile displays with good perceptual fidelity will require major advances in engineering, design, and fabrication. Research over several decades has highlighted the difficulties of meeting the required performance benchmarks using conventional devices, processes, and techniques. This has highlighted the important role that will be played by new material technologies that can bridge the electronic and mechanical domains. This must occur at the smallest scales, because of the great perceptual spatial and temporal acuity of the sense of touch. The requirements involved also furnish valuable performance benchmarks against which many emerging material technologies are being evaluated. This article highlights recent research and possibilities enabled through new material technologies, ranging from organic electronic materials, to carbon nanomaterials, and a variety of composites. Emerging material technologies are surveyed for the sense of touch, including sensory considerations and requirements, materials, actuation principles, and design and fabrication methods. A conclusion reflects on the main open challenges and future prospects for research in this area.

## 1. Introduction

The sense of touch is essential to most physical activities that sustain and enrich our lives. Human touch sensing is facilitated by resources spanning the nervous system, musculoskeletal system, and the skin, our largest sensory organ. Together, these comprise what is referred to as the haptic sense.

The sensory organ of touch is the skin. It is the largest organ of the body, comprising about 15% of our body mass.<sup>[1]</sup> It is a marvel of biological engineering, sensitive enough to detect

the footsteps of a fly, and strong enough to lift heavy suitcases. Skin is densely perfused by tactile sensory nerve endings and receptors—up to thousands per square centimeter. Together, they transduce a wealth of mechanical, thermal, or chemical inputs from the environment and body into sensory information. These signals enable us to perceive the objects and materials we touch, and how we touch them, and constitute an essential part of all of our physical actions.

In complexity and performance, the haptic perceptual system is comparable to vision and hearing. With it, we can immediately and easily discriminate huge varieties of fabrics according to texture, read braille books via touch, engrave delicate sculptures, grasp and strike a match, or perform delicate tasks using a needle. All of these become difficult to impossible if touch sensation is absent.<sup>[2]</sup> As a striking illustration of the great acuity of this system, consider that the finger, which is textured by millimeter-scale bumps and ridges is capable of discriminating surfaces that differ at the nanometer scale,<sup>[3]</sup> of detecting nanometer-scale vibrations,<sup>[4]</sup> and of locating micrometer-scale features on flat surfaces.<sup>[5]</sup>

The increasing integration of physical and digital environments in our daily activities has led to the development and proliferation of many technologies, from smartphones, to high definition televisions, and virtual and augmented reality displays. However, despite the involvement of touch contact in most real-world activities, information technologies for the sense of touch have largely lagged behind.

Tactile displays are devices for presenting dynamic tactile information to the skin. A longstanding engineering goal has been to realize tactile displays that emulate the sensations felt during natural touch interactions, much as video and audio displays are able to reproduce plausibly realistic audiovisual scenes. When compared with the latter, tactile display technologies are rudimentary. In fact, despite decades of research, all practical tactile display devices operate within narrow ranges. The best available technologies are limited to reproducing small arrays of pixels, such as Braille characters, and it is unclear how natural tactile experiences could be enabled with existing technologies. The reasons for this can be traced to the complexity of tactile signals, including distributed forces or displacements, and to the high spatial resolution, dynamic range, and temporal acuity of the tactile system. Technological challenges include the complexity of realizing micromechanical devices that can produce such signals.

---

Dr. S. Biswas  
California NanoSystems Institute  
Center for Polymers and Organic Solids  
University of California  
Santa Barbara, CA 93106, USA

Prof. Y. Visell  
Department of Electrical Computer Engineering  
Media Arts and Technology Program  
and Department of Mechanical Engineering  
California NanoSystems Institute  
Center for Polymers and Organic Solids  
University of California  
Santa Barbara, CA 93106, USA  
E-mail: yonvisell@ucsb.edu

 The ORCID identification number(s) for the author(s) of this article can be found under <https://doi.org/10.1002/admt.201900042>.

DOI: 10.1002/admt.201900042

The magnitude of these challenges is motivating growing research on new methods for the engineering, design, and fabrication of tactile displays that can match the capabilities of biological sensing. Conventional micro-electromechanical system (MEMS) technologies are inadequate for realizing general purpose tactile displays, due to the large amplitudes and large number of degrees of freedom involved. To see why this is true, consider the simpler category of special-purpose displays for reproducing Braille text. Braille consists of well-spaced dots that displace vertically by fixed heights of 0.5 mm. Even a small Braille display requires hundreds of moving elements to be packed in a space of a few square centimeters, and costs thousands of dollars. As explained below, the requirements of displaying Braille are orders of magnitude less demanding than what are required to emulate natural tactile signals.

Together, these considerations have led many groups to conclude that advances in material technologies, and methods for using them to engineer useful devices, are needed. The materials of choice for conventional MEMS devices—typically rigid materials—make it costly and challenging to realize large arrays of independently displacing elements. One way to mitigate such problems is to introduce flexible elements or soft materials, such as plastic films or soft polymers, that allow actuated elements to displace without sliding contact. In addition, haptics frequently involves intimate device contact with the soft skin of the body. This has motivated many researchers to focus on compliant materials, in order to improve comfort, ergonomics, or the efficiency with which mechanical energy is exchanged with the skin. A smaller, but growing, number of haptic devices are designed to be skin-conformable or stretchable, through the use of soft materials.

In addition to the widespread interest in realizing effective haptic displays, their engineering has also provided useful performance benchmarks against which emerging active material technologies can be measured, because of the large challenges and stringent performance requirements of tactile displays, as reviewed below.

The range of emerging material technologies that have been explored for using in engineering haptic devices is large and growing. It includes organic and inorganic soft materials, nanomaterials, functional fibers or textiles, liquid alloys, and composite materials. Emerging materials also integrate intrinsic functionalities of smart material transduction. Techniques for chemically synthesizing and doping these materials make it possible to greatly tune properties. Many materials of interest also integrate other attractive properties, including mechanical compliance or flexibility and optical transparency. The large range of emerging materials and properties are reflected in the diversity of the physical mechanisms of actuation that have been investigated. They include electrostatic, piezoelectric, electromagnetic, electrorheological, magnetorheological, liquid crystal, ionic, and fluidic actuation, among others, each with distinct advantages and disadvantages. Functional devices invariably also rely on new fabrication techniques and multiple materials. A wide range of the materials, actuation principles, design and fabrication techniques are reviewed here.

The next sections of this article are organized as follows. First, we review elements of the biological sense of touch in order to distill basic engineering performance requirements for



**Shantonu Biswas** is a post-doctoral fellow in the RE Touch Lab at the University of California, Santa Barbara, CA, USA. He received his Ph.D. degree (summa cum laude) from the Department of Nanotechnology at the Ilmenau University of Technology, Germany in 2018, where he developed a stretchable printed circuit board method and demonstrated first metamorphic electronic devices. He received his M.Sc. in Physics (nanoscience) from Lund University, Sweden in 2013 and B.Sc. in Physics from Shahjalal University of Science and Technology, Bangladesh. His research interests include flexible and stretchable electronics, wearable electronics, soft sensors and actuators, and additive manufacturing.



**Yon Visell** received his Ph.D. from McGill University (2011), and M.A. and B.A. degrees from University Texas-Austin and Wesleyan University. Since 2015, he is assistant professor in the department of Media Arts and Technology, Electrical and Computer Engineering, and Mechanical Engineering at the University of California, Santa Barbara, where he directs the RE Touch Lab. He was assistant professor (2012–2015) in the ECE department at Drexel University and post-doctoral fellow (2011–2012) at the Institute of Intelligent Systems and Robotics, Université Pierre et Marie Curie. He has been employed in industrial R&D. His research includes haptic mechanics, perception, engineering, and robotics.

tactile displays. Next, we discuss key categories of materials that have shown promise for realizing such displays, and review the physical actuation principles that are most often used. Because the devices of interest rely on unconventional materials, existing fabrication methods rarely suffice, as we review in the following section. The last part of this review surveys a wide array of the tactile display devices that have been realized using such techniques. We conclude with a discussion of open challenges, needed advances, and future prospects for this field.

## 2. Human Tactile Sensing: Biology, Perception, and Engineering Requirements

An electronic display, such as a video monitor or loudspeaker, is designed to match the characteristics of the sense modality, acting as a “mirror for the senses.” This helps ensure that what is displayed can be perceived, and that resources are not wasted

in displaying signals outside the perceivable range.<sup>[6]</sup> Examples of such signals are infrared light or ultrasound. Tactile display requirements must be informed by characteristics of biological touch sensors, tactile perceptual capabilities, and on the mechanical properties of the skin.

The haptic system, like other perceptual modalities, can be viewed as conveying several categories of information, including modality, location, intensity, and timing.<sup>[7]</sup> Especially prominent in haptics is the close involvement of two submodalities—those of sensing and movement—in nearly all natural perceptual experiences.<sup>[8]</sup> The first, touch sensing, involves the transduction and transmission of mechanical or thermal signals into impulses in the central nervous system. The second, movement, involves the displacement of the limbs or other body parts when touching an object. These movements provide the necessary context for the brain to use sensory information to perceive the world or interact with it.<sup>[2,9]</sup> This integrated view of haptic perception has facilitated scientific advances and guided the development of technologies for haptic feedback. A major challenge in haptic engineering is to realize general-purpose tactile displays for stimulating localized areas of the skin in ways that are similar to what is felt when touching real objects.

## 2.1. General Anatomy and Mechanics of the Tactile Sensory Organ

The sensory organ of touch is the skin. There are two main types of human skin. Hairy skin is thinner, and covers most of the surface of our body. Glabrous skin, which is thicker and hairless, covers the palmar surface of our hands, fingers, feet, and toes. Many tactile display technologies are designed to interface with glabrous skin, which covers the surfaces of the hands and feet that we use most when interacting with the external environment. Mechanically, glabrous skin is distinguished from hairy skin by its greater thickness, harder exterior (due to keratinization), and high stiffness under large displacements (due to collagen fiber reinforcement). Also distinguishing is the presence of epidermal ridges, or fingerprints. During tactile contact, the frictional properties of glabrous skin are dynamically altered by secretions from eccrine sweat glands. Such frictional phenomena are complex. To describe them would exceed the scope of this review.

The mechanical properties of the skin are nonlinear and largely vary among persons, skins, sexes, and ages.<sup>[10]</sup> Typically Young's modulus of skin from forearm is in the range of 1–10 kPa<sup>[11,12]</sup> which might increase to 15 MPa for forehead.<sup>[13]</sup> Stiffness of the hand tissues also varies. For instance, Young's modulus of stratum corneum, epidermis, and dermis are reported to be in the range of 2.5, 1, and 0.1 MPa, respectively.<sup>[14,15]</sup> However, it should be noted that the value of the Young's modulus largely depends on the measurement method used.

## 2.2. Sensory Receptors of Touch

The skin captures information about the external environment through receptors that are responsive to mechanical, thermal, and noxious (itchy or painful) stimuli.

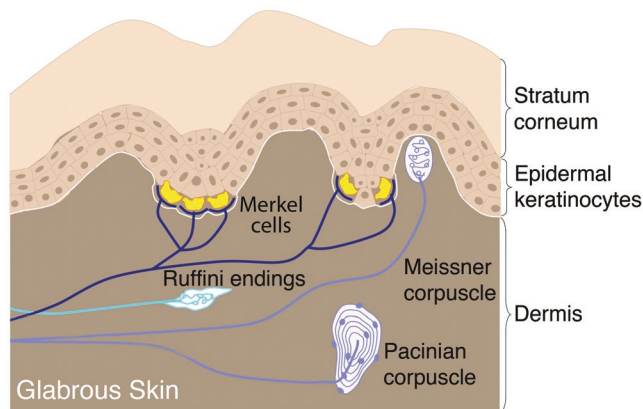


**Figure 1.** Schematic illustration of human tactile receptors in glabrous skin. Reproduced under the Creative Commons Attribution 3.0 License<sup>[16]</sup> Copyright 2016, the authors.

Glabrous skin of the hand possesses three main types of mechanical tactile receptor: Merkel disks (MD), Meissner corpuscles (MC), and Pacinian corpuscles (PC).<sup>[7]</sup> MD and MC receptors lie immediately below the epidermis, while PCs are situated in deeper tissues (Figure 1). MDs are the most numerous of tactile sensory receptors, reaching densities of  $500 \text{ cm}^{-2}$  or more in the glabrous skin of the fingertips. MCs are less numerous by a factor of 5. In adults, PCs number fewer than 1000 in each hand.<sup>[17,18]</sup> MDs and MCs are too small to be seen with the naked eye, whereas PCs are much larger, with lengths on the order of 1 mm. A fourth group of mechanical receptors, present in glabrous skin of humans but absent in many primates, are Ruffini corpuscles. They cluster around the nail in humans and act as stretch sensors.<sup>[18]</sup>

Each type of tactile receptor possesses an associated sensory neuron type. A single sensory neuron can innervate multiple receptors. Tactile sensory neurons extend from the skin through the spinal cord to the brain. This routing is called the medial lemniscal pathway.<sup>[7]</sup> Individual tactile neurons transmit information as action potentials, or spikes, to the brain, encoding the information necessary for perception. Tactile neurons associated with different receptor types respond differently to mechanical stimuli applied to the skin.<sup>[19]</sup> We summarize some properties of tactile receptors in Table 1. MDs produce sustained responses to static skin deformation. MCs and PCs are very sensitive to fast changes, including oscillating stimuli, and produce little output in response to static stimuli. The shallow locations of MC and MD receptors cause their responses to very low amplitude stimuli to be confined to nearby regions of skin because stimuli applied at larger distances yield sub-threshold strains at the receptor location. PCs are exquisitely sensitive, capable of responding to transient, nanometer-scale skin deformations. The skin efficiently transports transient or oscillating mechanical stimuli,<sup>[20]</sup> enabling individual PCs to respond to light contact over large areas of the hand.

Tactile receptor types can respond to oscillating stimuli applied to the skin within different frequency bands (Table 1). PCs respond over the widest frequency range, from tens of Hz up to nearly 1000 Hz depending on the stimulus amplitude and location.<sup>[26]</sup> For a wide amplitude and frequency range of such

**Table 1.** Summary of tactile receptor properties in human glabrous skin.<sup>[21–24]</sup> Such properties must be understood in light of complex amplitude- and stimulus-dependent response characteristics noted in the text. Multiple receptors may be innervated by the same nerve fiber, such that innervation densities can be lower by a factor of 1–10 or more.<sup>[25]</sup> Due to skin mechanics, touch contacts in even simple natural interactions elicit responses from multitudes of tactile neurons of all types.

Tactile receptor	Density, max. [cm <sup>-2</sup> ]	Response area at low amplitudes [mm]	Frequency range [Hz]	Preferred stimuli
Merkel disks (MD)	500+	0.5	0–100+	Slowly varying
Meissner corpuscles (MC)	100+	3–4	10–300+	Transient, oscillating
Ruffini corpuscles	10+	10+	0–300+	Sustained
Pacinian corpuscles (PC)	20+	20+	20–800+	Transient, oscillating

oscillating stimuli, individual PCs produce precisely one or two phase-locked spikes on every cycle of oscillation, irrespective of frequency and amplitude.<sup>[27]</sup> As the stimulus amplitude is increased, larger numbers of receptors respond. Thus, while it is common in the engineering literature to provide simplified descriptions of tactile receptors in terms of filter response characteristics, such a description is fundamentally flawed. Furthermore, touch contact in natural interactions elicits responses from numerous tactile receptors of all types.<sup>[2]</sup> These responses converge and are integrated at early stages of perceptual processing in the brain.<sup>[28]</sup>

### 2.3. From Sensation and Perception

The exquisite sensitivity of tactile receptors is reflected in perceptual abilities. A single spike from a tactile neuron is sufficient to elicit a conscious percept.<sup>[5]</sup> This capacity is thought to facilitate rapid detection and classification of tactile contacts in the brain.<sup>[2]</sup> Each tactile contact results in large volleys of such spikes being transmitted to the brain. Using these inputs, humans can perform remarkable feats of perception. They can distinguish textured surfaces with spatial structure at the nanometer scale.<sup>[3]</sup> When feeling an otherwise flat object, humans can locate raised surface elements less than a micrometer in height.<sup>[5]</sup> They can also effortlessly discriminate the textures of thousands of surfaces and materials,<sup>[18]</sup> such as the many textiles in a fabric store.

### 2.4. Implications for Tactile Display Design

From the foregoing discussions, an idealized tactile display matching the organization and capabilities of the tactile sense could be considered to require spatial resolutions approaching the micrometer scale. For a tactile display with dimensions of 1 cm × 1 cm, this would demand an array on the order of 10 000 × 10 000 moving elements packed in an area of 1 cm<sup>2</sup>. Because the range of tactile displacements we are sensitive to is large (from about 10<sup>-6</sup> to 10<sup>-3</sup> m), each such unit should be capable of displacing by 1 mm or more (even if the relative displacement of adjacent units can be constrained to a smaller value). To match the maximum tactile temporal resolution, such a display would also need to possess a bandwidth approaching 1000 Hz. If worn on the finger, or mounted as a fixed display on a surface, such a device could simulate a vast array of surfaces, objects, and materials with

reasonable perceptual fidelity, providing a tactile analog to a high-definition television.

Today, however, no device or technology can come close to meeting such requirements, and the shortcomings amount to several orders of magnitude. While this gap may require research over many years to be fully bridged, tactile capabilities are limited in other ways that can simplify the engineering of practical displays. For example, distinct tactile subsystems are associated with high temporal resolution (PC receptors) and high spatial acuity (MD receptors).<sup>[29]</sup> This could enable a decomposition of engineering devices into high frequency and high spatial resolution subsystems. Further, while the requirements for an idealized display are daunting, a comparison may be drawn with the history of video technologies. Video displays of lower resolution than human visual acuity, and of more limited dynamic range, have enabled compelling experiences, which have been used in applications from cinema to virtual reality. Other limitations in perceptual processing are reflected in perceptual equivalencies and in tactile illusions.<sup>[30]</sup> These often point to potential strategies for tactile display design. Nonetheless, the large gap between existing technological capabilities and tactile perceptual abilities indicates that new technologies and engineering approaches are needed, and among the most promising are emerging material technologies.

## 3. Emerging Materials for Haptic Devices

The challenges of realizing a general-purpose tactile display are now recognized by a growing cadre of researchers. The required capabilities exceed what is possible with conventional devices, such as MEMS. Consequently, there is an increasing interest of new material technologies that might overcome these difficulties.<sup>[31–34]</sup> Motivation for this interest has also been driven by the large contemporary research activity in materials science and engineering.

For last couple of decades, the material engineers have added a new direction in their research that expanded from developing bulk materials to realizing smart functional materials. This expansion is due to the limitations of the conventional electronic materials since next generation devices will require advanced functionalities such as mechanical flexibility or transparency that is no longer possible to achieve using conventional materials. Moreover, smart materials such as some polymers demonstrate functionalities that cannot be observed in, for instance, Si-based devices.

Another important aspect of introducing new materials type is technology related, i.e., scaling effect. To give an example, Si-based electronic devices are typically limited by their size. Till this day, no technology exists that is capable of producing continuous devices in large scale or roll-to-roll manner using conventional rigid materials such as Si, which is highly demanding nowadays. On the other hand, required technology to realize polymer based devices often can be large scale or roll-to-roll. Moreover, processing of polymers is simple and cost-effective, and typically environment friendly.

Considering these issues, engineers have developed a large number of smart materials with desired functionalities. In the following sections we will review some of the emerging materials which have been widely used to realize haptic devices.

### 3.1. Soft Materials

A key reason that many soft materials have been considered to be well suited for tactile displays is their mechanical compliance. Tactile displays comprise interfaces with the skin. Skin is mechanically soft compared to many conventional devices made from rigid and brittle materials. A display that can match the compliance of the skin may improve mechanical transmission, and aid ergonomic comfort.<sup>[35,36]</sup> Furthermore, many examples in nature demonstrate how novel functionality can be enabled through the use of soft materials, rather than the hard materials of conventional mechatronic systems. Soft materials include liquids, gels, colloids, polymers, foams, and biological tissues. While an important class of these materials involves polymers, many inorganic materials also fall in this category. They include water, ionic solutions, and eutectic metal alloys—metal conductors that are liquid at low temperatures.<sup>[32,35,37–43]</sup>

Natural rubber is a material that has been used since ancient times, including many early robotic and sensing applications.<sup>[44,45]</sup> Synthetic polymers, such as silicone elastomers, can have tunable properties. They have been widely used for daily products such as food packaging, surface coating, and medical components, and are increasingly used in intrinsically soft electronics, sensors, and actuators, including tactile display devices.<sup>[46,47]</sup>

### 3.2. Organic Materials

An especially relevant area of research in materials science and engineering is connected to advances in organic materials. This category of materials includes many that, alone or in composites, can be used to realize actuators suited for tactile display applications. Organic materials have several properties that make them attractive for realizing actuated devices.<sup>[36,48]</sup> They can be designed and synthesized to have properties that are matched to application needs. They can often be processed in solution, aiding large surface area applications. Some of them possess, or can be endowed with, attractive properties including electronic or ionic functionality, flexibility or stretchability, and self-healing. They can be patterned and formed into functional composites using a

growing library of techniques, including photolithography, laser micromachining, and many other methods, as reviewed below (Section 5).

### 3.3. Emerging Nanomaterials

One of the most popular emerging materials for device technology is nanomaterials. The physical properties of the materials in nanoscale vary largely from the bulk and can be controlled very precisely which is essential to achieve high performance devices. Graphene is one of the examples of nanomaterials that has been widely investigated and used for high performance devices since it shows high conductivity and mechanical flexibility, and at the same time it can be transparent.<sup>[49,50]</sup> Other nanomaterials such as nanoparticles, nanowires, thin film have been used to realize haptic devices. For example, nanoparticles and nanowires are often mixed with polymers to increase the dielectric property or conductivity of the materials to realize functional haptic devices.<sup>[51–53]</sup> Carbon nanotubes (CNTs) and black carbon also have been used in similar manner to demonstrate functional haptic devices.<sup>[54]</sup>

There are also polymer based nanomaterials showing exceptional properties that are absent in the bulk. For example, nanoporous or mesoporous polymer materials show extremely high specific areas compared to the bulk that can influence the device performance.<sup>[55–57]</sup>

### 3.4. Composite Materials

Another emerging area of research comprises functional composite materials, including textiles and fabrics. While functional fabrics have been available for decades, only recently have integrated textile devices become possible, and there is growing interest in new methods for using them to produce working devices and systems, including electronics.<sup>[58]</sup>

There are a wide range of liquid materials that have been used to realize functional haptic devices. These include liquid alloy, rheological fluids,<sup>[59,60]</sup> liquid crystals,<sup>[61,62]</sup> and gels.<sup>[63,64]</sup> Many of these emerging materials demonstrate special functionality which is preferable for some particular applications. For example, electrorheological fluid (ERF) and magnetorheological fluid (MRF) are two rheological fluids that change their viscosity based on applied electric or magnetic field, respectively. Moreover, most of these composite liquids are often realized by mixing different materials which also provides additional degrees of freedom to modify the material properties.

There are other nonconventional materials that have been used to demonstrate haptic devices such as electroactive paper (EAPap).<sup>[53]</sup> A short list of examples of haptic devices based on emerging materials has been summarized in Table 4. Unique properties and functionalities of these individual or composite materials enable wide range of actuation mechanisms which is essential to realize functional haptic devices. In the next sections we will discuss different actuation principle based on these emerging materials.

## 4. Physical Principles of Actuation via Emerging Materials

An actuator is a transducer from an input energy source into mechanical energy resulting in a displacement (strain), or forces (stresses). Occasionally, the term actuator is also used to describe thermal output devices. Actuators are thus an essential element of any tactile display. They can be characterized by the source of input power (commonly electrical, mechanical, or thermal) and physical means of conversion to mechanical energy. They exert forces on the human body, or exchange heat, to stimulate the tactile sense.<sup>[65]</sup> Many actuation mechanisms have been adapted to realize tactile displays. This review is focused on emerging material technologies. As such, more established technologies, including electric motors, shape-memory alloys, and many others, are not reviewed, as these are well-covered in other articles and textbooks.

### 4.1. Fluid-Driven Elastic Polymers

Among the simplest applications of polymer materials in haptic actuators are fluid-driven devices. Fluid-driven actuators use a working fluid to transfer energy from source to the device, through the application of pressure or volume change. The choice of fluid depends on application needs. Compressible fluids, such as air, are lightweight and low viscous. However, they can be slow to respond, and can require good sensing and control in order to compensate for dynamics and losses. Incompressible fluids, such as water or oil, are amenable to producing large forces, and to actuating at high speeds. However, incompressible fluids have higher viscosity, and are heavier.<sup>[66–68]</sup> The rapid pressure losses that result from reductions in volume can make them difficult to control. A large variety of fluid-driven actuators has been developed. Soft fluidic actuators are also typically patterned so as to differentiate the effective stiffness in selected areas.

Here, we confine our discussion to fluid-driven actuators for haptic devices, including tactile displays. A major category of these devices consists of pneumatic or hydraulically actuated silicone elastomer structures. In this section, we also briefly discuss broader applications in haptics, which involve the delivery of vibration, compression, or strain to large areas of the human skin, often at lower resolutions than are needed for tactile display.

#### 4.1.1. Compressible Fluids

In practice, all fluids are compressible to some degree. Here, we focus on gases, such as air, which is arguably the basis of the most widely used soft actuators. Air actuators are also called pneumatic actuators. They use positive or negative pressure to transfer energy and to perform mechanical work. Pneumatic actuators produce strain via the movement of fluid within a cavity. Fluid motion may be produced through the motion of a piston, pump, or bellow, yielding linear motion, or (less commonly) rotational motion.

A detailed physical modeling of a pneumatic actuator requires in-depth analysis of the entire system, which creates complexities. Generally, compressible fluids are governed by the ideal gas law,  $pV = nRT$ , where,  $p$ ,  $V$ , and  $T$  are the pressure, volume, and temperature, respectively. A consequence of this is the relation for a closed system,  $n = \text{constant}$ , near thermodynamic equilibrium one has

$$\frac{p_1 V_1}{T_1} = \frac{p_2 V_2}{T_2} \quad (1)$$

where, the subscripts 1 and 2 refer to two different states equilibrium of the system. The total energy of the system for a quasi-steady state flow of any incompressible fluid is conserved. Sources of energy include kinetic energy, potential energy, and thermodynamic energy, which involves entropy and heat exchange. Energy conservation implies that sum of these terms is constant. This conservation principle can be expressed through Bernoulli's equation

$$\frac{v^2}{2} + \psi + \epsilon + \frac{p}{\rho} = \text{constant} \quad (2)$$

where,  $v$  is the fluid velocity,  $\rho$  is the density,  $\psi$  is the potential energy, and  $\epsilon$  is the thermodynamic energy, all expressed per unit mass of the fluid. The last two terms in this equation constitute the enthalpy of the system. Alone, these equations are not sufficient to model pneumatic actuators, as energy exchange with other system elements and the environment must be accounted for.

Many fluidic actuators have been proposed based on flexible or stretchable polymer structures. They comprise two main groups: balloon-based and thin film-based actuation. Thin film-based actuators consist of flexible or stretchable films charged with air. These films may be enclosed, or laminated or bonded onto a stiffer silicone, fabrics, or other material. They expand or collapse depending on the applied pressure and any stiffness constraint arising from the composite structure. Balloon actuators, in contrast, can operate in several different modes, including bending, twisting, or elongation. This is possible due to their asymmetric shape, which can be altered through composite structures with varying stiffness. Such fluidic actuators can be operated in different modes, including suction, or negative pressure, pressure-induced bending, twisting, expanding, and transiently via vortices.

The most common materials used in fluidic actuators for haptic applications are soft silicone elastomers, such as poly-dimethylsiloxane (PDMS) and platinum catalyzed silicone elastomer (for example, EcoFlex, Smooth-On Inc., Easton, PA, USA). One popular approach for the fabrication of such devices is based on mold casting. In these processes, liquid silicone is cast, cured, and bonded to a 3D mold in order to create internal hollow channels for the actuator. 3D printing of silicone elastomers is also used to alter and speed up the fabrication. The operating rates of the pneumatic actuators are typically governed by the working pressure, which, together with the device structure, determines the effective stiffness,  $k$ , of the medium. Working pressure limits are determined by the elasticity of the

structure, and from safety considerations. Typical frequencies are 20–30 Hz.<sup>[72,73]</sup>

Pressure-driven pneumatic actuators have been used by several groups to realize soft actuated devices for haptics. As a simple example, the wearable, restricted-aperture pneumatics (WRAP) system of Raitor et al. consisted of wearable technologies with applications to haptic guidance.<sup>[69]</sup> The system comprised a thin, flexible polymer cavity with two ports, an inlet and a vent (Figure 2A). Absent positive pressure, the actuator remains in an uninflated condition. When a positive pressure is applied through the inlet, the actuator is inflated, exerting a pressure on the skin. Of greater interest to the present review are pneumatic tactile display devices, such as that created by Russomanno et al. (Figure 2B), which provide active tactile feedback.<sup>[70]</sup> The actuators contain thin elastic membranes comprising cavities that deflect upward, creating surface features when the cavity is pressurized.

Several examples of pneumatically driven tactile actuators are reviewed in Section 6, below. Some of those that have been developed include soft tactile displays<sup>[74–77]</sup> including pneumatic logic circuits with integrated switching.<sup>[78]</sup> Also related to these are soft grippers<sup>[79,80]</sup> or soft robotics.<sup>[81–84]</sup>

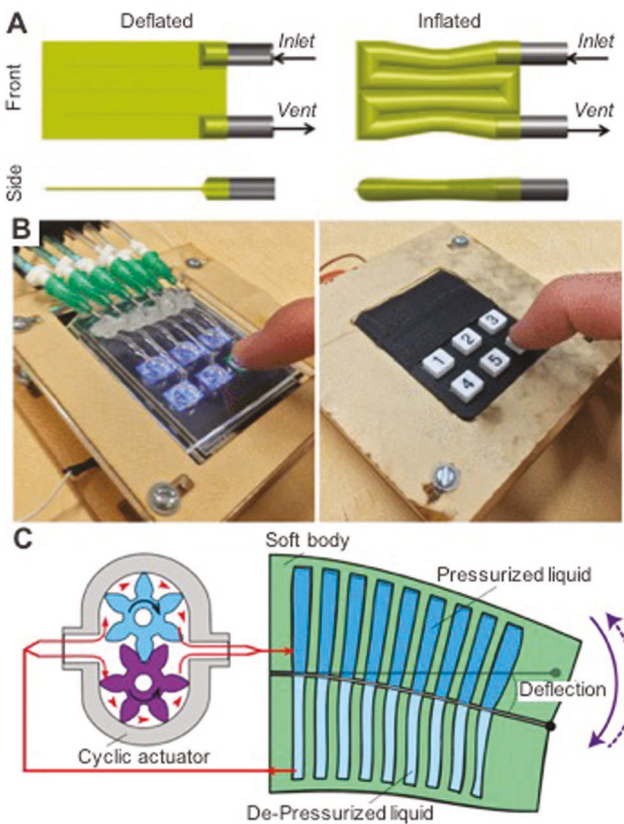


**Figure 2.** Demonstrations of pneumatic actuators based on soft materials. A) A general operation mechanism of a pneumatic actuator. Reproduced with permission.<sup>[69]</sup> Copyright 2017, IEEE. B) Photographs of a tactile feedback device based on pneumatic actuation. Reproduced with permission.<sup>[70]</sup> Copyright 2017, IEEE. C) An example of a hydraulic actuator showing a general operation mechanism. Pressurized liquid leads to stretching a part of the soft body that leads an undulating motion. Reproduced with permission.<sup>[71]</sup> Copyright 2016, IEEE.

The pneumatic actuators are usually simple, do not require sophisticated mechanisms, and can achieve high moving speed. Additionally, these actuators are usually cheap and can be ecofriendly and biocompatible. On the other hand, since pneumatic actuators use compressible air, the applications are limited, function at low bandwidth, and show hysteresis during cycles.

#### 4.1.2. Incompressible Fluids

Actuators using incompressible fluid often employ water or oils as working media. These are referred to as hydraulic actuators. The physical principles of actuation for such devices are similar to those of pneumatic actuators. The incompressibility of the working fluid prevents input energy from being stored in the driven fluid. This can provide energetic advantages in some regimes, and facilitate their application for providing higher forces. However, in high-speed applications, viscous losses can become important. When channels are narrow, capillary forces must be accounted for.

Hydraulic actuators often rely on an effect described by Pascal's law to amplify forces,  $F$ , in response to input pressures,  $p$ . This relation states that  $F = p \times A$ , where  $A$  is the effective area of the fluid. When the area in different regions of a device differs, a difference in forces is produced when  $p$  is constant. To draw an illustration, let us imagine a hydraulic tube with different areas, say  $A_1$  and  $A_2$ . If  $A_1 < A_2$ , for a constant applied pressure  $p$  the corresponding force  $F_2$  will be higher than the  $F_1$ . Such a system also obeys Bernoulli's Equation (2).

A simple example of a hydraulic actuator system consists of a cylindrical actuator controlling the flow of a driving liquid, like that proposed by Katzschmann et al. (Figure 2C). The liquid can, in turn, actuate a soft actuator to produce physical deformation.<sup>[71]</sup> In this device, the soft actuator is pressurized, and the soft body stretches while the complement remains unstretched. This produces an undulating motion. There are many other examples of soft actuators based on hydraulic actuation principles. These have found applications on soft grippers,<sup>[40]</sup> soft robotics,<sup>[71,85]</sup> artificial muscles,<sup>[41,86,87]</sup> and training,<sup>[88]</sup> among others. However, relatively fewer soft haptic actuators have been developed based on such principles.<sup>[89]</sup> An example of such a system that was used to realize a simplified tactile display is given in Section 6.

Unlike the pneumatic actuators, hydraulic actuators can achieve the high bandwidths necessary for high performance tactile displays. They can also produce high power, but can be sensitive to rheology or chemistry of the working liquids. In addition, they may require careful design and maintenance. Since, hydraulic actuators use incompressible fluids, in some operating regimes—notably, low-speed flow—little input energy is lost, providing efficient energy transmission.

#### 4.2. Electrostatic Actuation

Electrostatic actuation has been widely investigated for use in emerging material actuators. These methods have received considerable attention due to the simple electronic controllability

they offer, since the source of power is an electric voltage or current. The simplest example of such a device relies on electrostatic Coulomb forces generated by two charged bodies.<sup>[90,91]</sup> An elastic dielectric material intervenes between the bodies providing a mean for transforming electrostatic energy into mechanical energy and physical deformation. To facilitate such displacements, soft polymers are often used.

Polymer actuators for converting electrostatic energy to mechanical energy have been described by several names in the literature. Nomenclature in the literature is not always consistently applied. The term dielectric polymer actuators emphasizes the elastic property of the dielectric medium. The term electroactive polymers has also been used to describe these devices, in addition to others that may involve charge transport through an ionically or electronically conducting polymer. Another category of polymer actuators based on the application of an electric field comprises piezoelectric polymers. Other actuators operate based on ion charge transport in a compliant medium, and may also be included in this category. Together, these actuators have attracted the attention of researchers working in a variety of areas. They have been described as forms of artificial muscles,<sup>[92]</sup> although for the purpose of this survey the most important attributes are related to their suitability as emerging technologies for haptic devices.

#### 4.2.1. Electronic Polymer Actuators (EAPs)

Electronic EAPs are also known as dry EAPs and activated by an electric field. In order to produce large strains, many EAPs require large electric fields of several kilovolts per millimeter. Because of the limited flow of bulk material, these actuators can be designed to operate very quickly, actuating within 1 ms or less. Moreover, such devices can be stable at room temperature, and can be designed to produce large forces (albeit at large voltages). Several subtypes of actuators exist in this category.

**Dielectric Polymer Actuators (DEAP):** The basic working principle of an electronic EAP consists of a polymer sandwiched between two electrodes (see Figure 3A). If a high voltage is applied to the electrodes, the Coulomb attractive force squeezes the polymer, which results in an increase in area, and concomitant strains, depending on the geometry of the assembled device. The volume of the DEAP remains nearly same before and after deformation. If a voltage  $V$  is applied between two electrodes separated by a DEAP with thickness  $d$ , the effective compressive stress of the polymer  $p$  will be<sup>[93]</sup>

$$p = \epsilon \epsilon_0 (V/d)^2 \quad (3)$$

where,  $\epsilon$  is the relative dielectric constant of the polymer and  $\epsilon_0$  is the dielectric permittivity of free space,  $8.85 \times 10^{-12} \text{ F m}^{-1}$ .<sup>[94]</sup> The value  $\epsilon$  reflects the polarizability of the material upon applying an electric field. A higher value of  $\epsilon$  means that the material has a higher polarizability which will result in a higher  $p$ . Typically, materials with high dielectric constant are preferable to achieve a higher mechanical strain or stress. A detailed model of the performance of such a device must also account

for the thermodynamic mechanisms of stress production in the elastomer.<sup>[93]</sup>

The expansion of the DEAP under electrical bias can be used to realize devices that can produce local deformation in different shapes. For example, Kim et al. used a DEAP sandwiched between two graphene electrodes as shown schematically in Figure 3B,C.<sup>[50]</sup> The cross-sectional view of the device and operation principle shows that, with this geometry, the polymer overlapped by the electrodes deforms to a convex shape (a bump) when an electric voltage is applied to the electrodes. A sufficiently large deformation can be used within a tactile display which demands materials with a low Young's modulus.

Various dielectric polymers have been developed based on silicone,<sup>[43]</sup> polyurethane,<sup>[93]</sup> acrylic,<sup>[95]</sup> or other materials. These materials have been used to demonstrate numerous haptic feedback devices.<sup>[96–100]</sup>

Mechanical strains greater than 100% are achievable using DEAPs. Because the effect is electrostatic, the response time can be fast, on the order of millisecond.<sup>[101]</sup> DEAPs can be constructed from dielectric elastomer materials that can achieve strains of up to 300%, such as the commercially available acrylic elastomer VHB 4910 (3M). DEAPs generating strains of 1692% have been reported by Keplinger et al.<sup>[95]</sup> using such an acrylic membrane.

In general, DEAPs show high mechanical energy density which results in relatively large actuation force.<sup>[94]</sup> Moreover these actuators have a long life under normal conditions. However, performance of DEAP actuators is also limited by the mechanical and electrical breakdown voltages, or field strengths ( $100 \text{ MV m}^{-1}$ ), above which the dielectric acts as a conductor.<sup>[101,102]</sup>

**Electroadhesive Devices:** When a dry human finger slides over a conductive electrode coated with a dielectric material, an increase of friction is observed when a voltage is applied to the electrode. The effect disappears when the voltage is removed. The AC version of this induced friction effect has been referred to as electrovibration.<sup>[103]</sup> This variation of friction surface by applying a charge to the finger has been shown to be an efficient method of inducing haptic sensations between a sliding human finger and touched surface, and has been used to realize tactile displays for rendering surface textures. AC voltages are preferred because the changes in friction are more easily felt, and because a DC voltage can cause charge to accumulate on the surface of the insulator, reducing the extent of the effect via charge shielding. When a sufficiently high voltage is applied, the attraction force becomes larger, generating normal forces on the finger that elicit a large enough change in friction to be felt.<sup>[104–107]</sup>

The electrostatic force ( $F$ ) generated in between the rubbing finger and the electrode is governed by Coulomb attraction, as in a DEAP device

$$F = \frac{A \epsilon \epsilon_0}{2} \left( \frac{V}{d} \right)^2 \quad (4)$$

where,  $A$  is the contact area of the fingertip,  $\epsilon$  is the relative dielectric constant of the stratum corneum,  $\epsilon_0$  is the dielectric permittivity in the free space,  $V$  is the applied voltage, and  $d$  is the thickness of the stratum corneum.<sup>[108]</sup> The method is

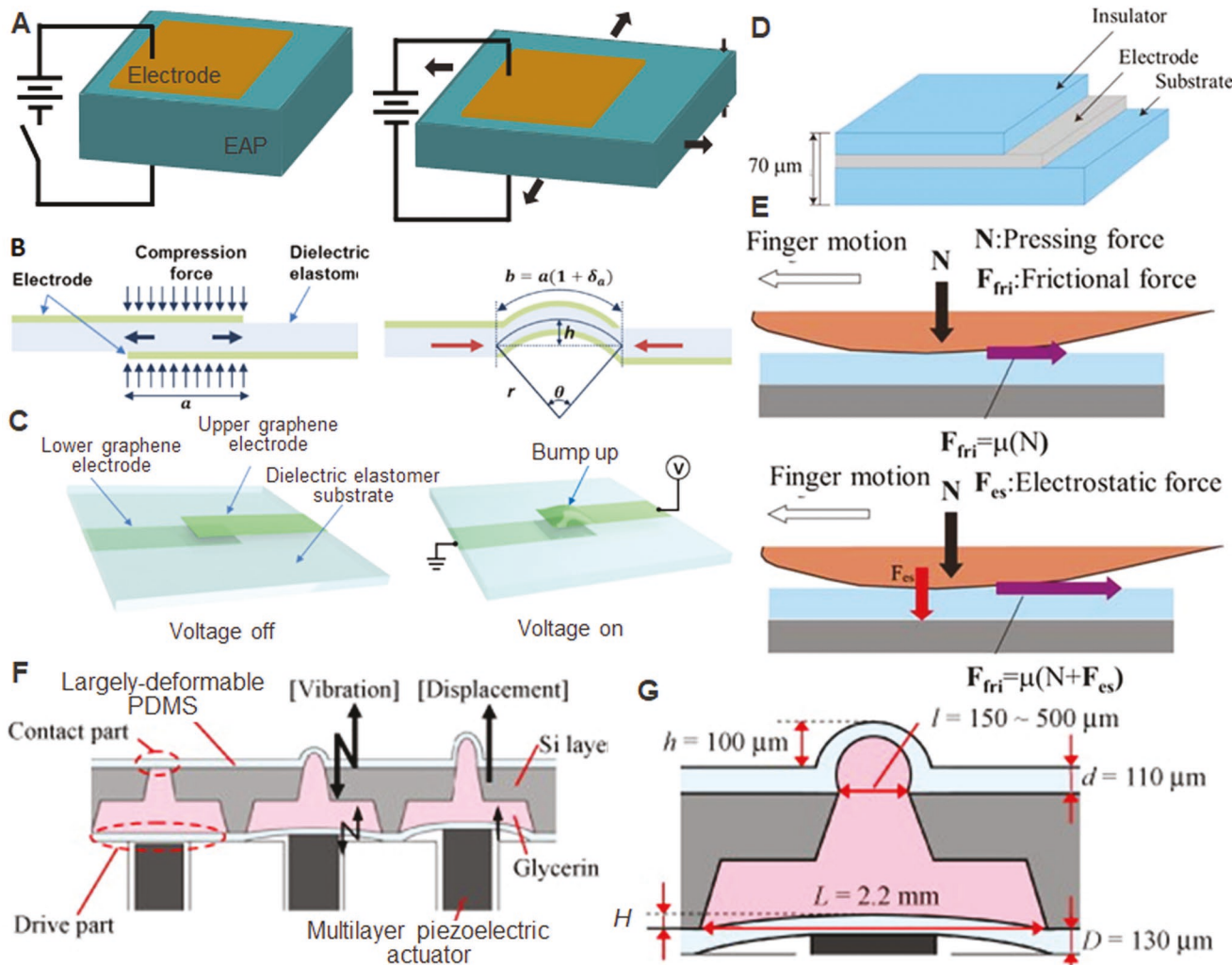


**Figure 3.** A) Schematic illustration of actuation principle of electronic EAPs. When an electric field is applied to a sandwiched electronic EAP between two electrodes, the polymer squeezes due to the Coulomb force. B) Operation principle of a practical actuator based on electronic EAP and C) the design of such a device. A dielectric EAP is sandwiched in between two electrodes (left) and the expansion of the polymer in the overlapping region is used to form a bump. B,C) Reproduced with permission.<sup>[50]</sup> Copyright 2013, IOP Publishing Ltd. D) Conceptual design and diagram of the electrostatic tactile display and E) operation principle of such tactile display. An electrostatic force is generated in between rubbing finger and insulator while applying a high voltage to the electrode. D,E) Reproduced under the Creative Commons Attribution License CC BY 4.0.<sup>[110]</sup> Copyright 2018, the authors. F) Schematic cross-sectional view and operation principle of a tactile display using multilayer piezoelectric actuator. When the piezoelectric actuator expands under an electric bias, it deforms and pushes the sealed liquid on top. G) Schematic design and different layers of materials in the tactile display. F,G) Reproduced with permission.<sup>[111]</sup> Copyright 2009, Elsevier B.V.

particularly favorable for applications where the device requires to be thin, transparent, and flexible since the method requires a single layer of insulator and a single layer of conductor which can be thin and transparent. Additionally, no moving mechanical parts are required in order to operate the device. However, the performance of the device depends on the thickness of dielectric layers, dielectric constant of the materials, and the applied voltage.

An example of a tactile device based on electrostatic adhesion and their general operation principle are schematically shown in Figure 3D,E. Schematic device layer (D) shows that an electrode is covered with a thin insulating layer. A thin layer of PDMS was used on top of the poly(3,4-ethylenedioxothiophene) polystyrene sulfonate (PEDOT/PSS) electrode

as an insulating layer; while a high voltage was applied to the electrode, the insulator was charged positively. When a finger was rubbed (Figure 3E) on the insulator, the finger became negatively charged which resulted in an electrostatic force which was felt as tactile sensation or surface texture to the user. Electroadhesion method has also been widely used in haptic rendering<sup>[109]</sup> and tactile displays,<sup>[106,107]</sup> to give a few more examples.

**Johnsen–Rahbek Effect:** A similar but larger attractive force occurs when an electric field is applied across the boundary between a conducting and a semiconducting surfaces and this effect is known as the Johnsen–Rahbek effect. The resultant attractive force depends on the applied voltage and on the materials involved.<sup>[112]</sup> One effective model of the produced

attraction force,  $F_e$ , was proposed by Atkinson<sup>[112]</sup> and can be described in simplified form as

$$F_e = \int_0^r \frac{V^2 r}{4d^2} dr \quad (5)$$

where,  $V$  is the applied potential across the boundary,  $d$  is the distance between the surfaces, and  $r$  is the radius of the contact point with a width of  $dr$ , say a region of fingertip skin. This effect have been used to realize tactile surface textures and actuators.<sup>[103,113]</sup>

**Piezoelectric Actuators:** The piezoelectric effect arises when a mechanical force or pressure is applied to certain materials, yielding electric charge flow. This is called direct piezoelectric effect. It is a reversible process and the reverse mechanism of this is known as inverse piezoelectric effect. While an electric field is applied to a piezoelectric material, it changes shape. This is a result of mechanical displacement of the charges in the materials due to the applied bias.<sup>[114]</sup> The physical deformation happens along the crystal orientation and is anisotropic. Thus, in contrast to the simplified description below, tensorial models are required to fully describe piezoelectric transduction. Such a physical deformation of the material can be used to generate tactile sensations.

In principle, all piezomaterials have resonant frequencies. Below such a frequency, such a device acts as a capacitor. A simple relationship between the current,  $i$ , and the voltage,  $V$ , of a piezoactuator is thus given by

$$i = C \frac{dV}{dt} \quad (6)$$

where,  $C$  is the capacitance of the device

$$C = n\epsilon \frac{A}{d} \quad (7)$$

where,  $A$  is the surface area of the electrode,  $d$  and  $\epsilon$  are the thickness and dielectric constant of the piezoelectric material, respectively, and  $n$  is the number of piezolayers in the device. In general, a tensorial relationship between mechanical and electrical deformation is involved.<sup>[115,116]</sup> Piezoelectric actuation method has been widely used in haptic devices,<sup>[117–120]</sup> to give a few examples.

**Piezoceramics:** There are a number of piezoelectric materials available including both organic and inorganic materials. A few examples of inorganic piezoelectric materials are lead zirconate titanate (PZT,  $Pb[Zr_xTi_{(1-x)}]O_3$ ), lead titanate ( $PbTiO_3$ ), AlN,  $ZnO$ ,  $Pb(Mg_{1/3}Nb_{2/3})O_3$ – $PbTiO_3$  (PMN–PT), quartz, berlinitite ( $AlPO_4$ ), potassium sodium tartrate tetrahydrate (rochelle salt), etc. Multilayer piezoelectric ceramics are often used to generate larger effects, such as are needed for tactile displays, but this requires greater current to be supplied.<sup>[121]</sup> The reverse-piezoelectric effect can be used for tactile sensing.<sup>[122]</sup> For example, Dagviren et al. developed a conformal piezoelectric system based on PZT that could actuate and sense.<sup>[123]</sup> This thin device used an elastomer as a substrate material and meander-shaped metal traces for electrical connections. As an active layer, they used 500 nm thick PZT material sandwiched between Pt and

Au electrodes encapsulated by polyimide (PI). When a voltage is applied to one of the actuators, it expands six to eight orders of magnitude more than the other elements in the circuit. Several other examples of actuators and motors using piezoelectric materials have been applied for haptic feedback.<sup>[124,125]</sup>

**Piezoelectric Polymers:** There are also several piezoelectric polymers which vary in their structures and mechanisms. For examples, poly(vinylidene fluoride) (PVDF), polyamides, parylene-C are semicrystalline while polyimide, polyvinylidene chloride (PVDC) are amorphous piezoelectric polymers. The first type arranges positively and negatively charged ions in crystalline form when an electric field is applied. The latter type contains molecular dipoles in its molecular structure. The dipole of this polymer is aligned when electric field is applied above a glass transition temperature. There are also examples of composite piezoelectric polymers where inorganic piezoelectric materials are combined with polymers. This results in higher coupling factors and increased dielectric constants, with a controllable mechanical flexibility. Another type of piezoelectric polymer, known as voided charge polymers, contains gas voids in its structure. When an electric field is applied to this polymer, gas voids become electrically charged resulting in a piezoelectric effect.

One example of a tactile display based on piezoelectric material was demonstrated by Ninomiya et al. (Figure 3F,G). The authors filled a chamber with an incompressible liquid that could be compressed using a multilayer piezoelectric actuator placed beneath the chamber. When an electric bias is applied to the piezoelectric materials, it expands and pushes the membrane upward.<sup>[111]</sup> Another example of a tactile stimulator based on piezoelectric polymer was demonstrated by Akhter et al.<sup>[126]</sup> In their device, a PVDF film based resonating actuator was coupled with a PI chamber. 80  $\mu m$  thick PVDF film was sandwiched between two 100 nm thick Ag electrodes. The final device comprised a  $3 \times 4$  actuated dot array in a PI membrane. The actuated dots could perform 257 nm displacement with 339  $N m^{-2}$  pressure, which is marginally in the range perceivable by the tactile sense. The response time of the stimulators was 0.7 ms with an input voltage of 80 V. Several other examples of soft tactile actuators based on piezoelectric materials have also been developed.<sup>[126,127]</sup>

#### 4.2.2. Ionic Polymer Actuators

Ionic EAPs, also known as wet EAPs, operate based on ion diffusion induced by an electric field. These types of polymers contain anions or cations which are bonded within their structure (see Figure 4A). Similar to the electronic EAPs, ionic EAPs are also sandwiched between two electrodes. Without any applied bias the ions are randomly distributed within the polymers which diffuse through the membranes while a bias is applied. The diffusion of the ions depends on the applied bias and on the ion concentration in the polymers. This ionic mass transformation results in expansion or contraction in the polymer, driven by the ions. Though a small bias voltage is required, a higher electrical power and energy is needed to achieve performance suited for tactile display. Such actuators have slow response time, but are able to produce large bending

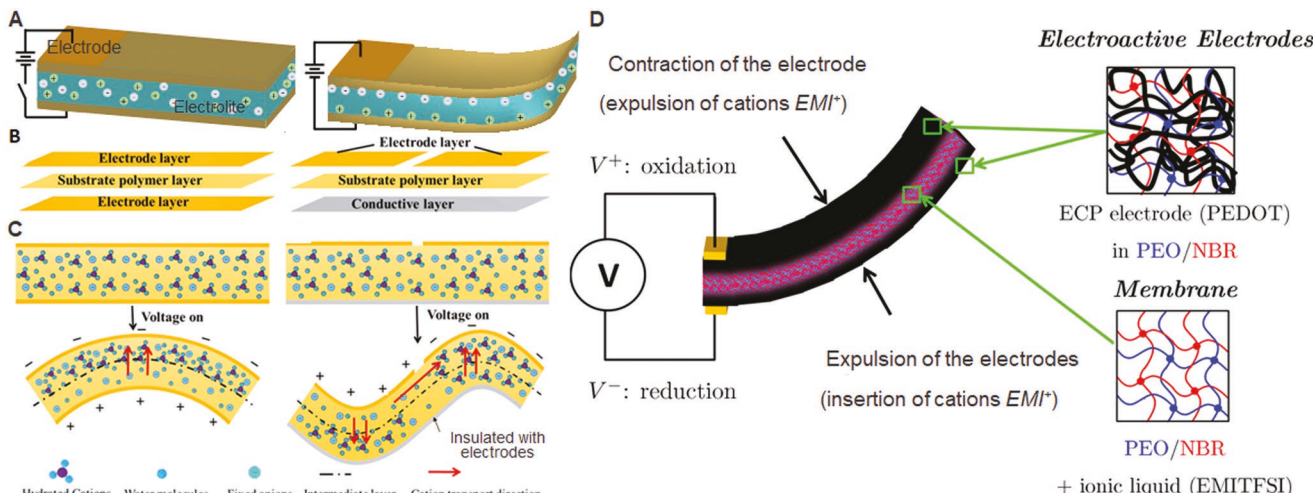


**Figure 4.** A) Illustration of the actuation principle of an ionic EAP. Ionic diffusion is used to actuate the ionic EAPs while a voltage is applied to the attached electrodes. B) Schematic design of a practical actuators based on ionic EAP's and C) operation principle of the device. While a voltage is applied to the electrodes, the ions diffused to the electrodes which leads to the bending of the polymer. B,C) Reproduced with permission.<sup>[128]</sup> Copyright 2018, IOP Publishing Ltd. D) Design of a polymer actuator based on conducting interpenetrating polymer networks (C-IPNs) and their composites. Reproduced with permission.<sup>[134]</sup> Copyright 2003, WILEY-VCH Verlag GmbH and Co. KGaA, Weinheim.

or displacements. This polymer type includes ion polymer metal composites (IPMC), conducting polymers, electroactive gels, and electrorheological fluids.

**Ionic Polymer–Metal Composites (IPMCs):** IPMCs are a composite of ionic polymer and conductive medium, and have often been referred to colloquially as “artificial muscles” (although biological muscles operate based on very different principles). The active portion of these devices consists of a polyelectrolyte membrane sandwiched in between two electrodes. Typically, the polyelectrolyte membrane is treated such that it is permeable to cations while impermeable to anions. The surface of the polyelectrolyte is usually coated with a thin metal layer to increase the surface conductivity. To increase the ion concentration of the electrolyte, the polymer is often mixed with highly conductive nanoparticles such as Pt or Au. When an electric bias is applied to the electrodes, the cations drift toward the cathode resulting in a swelling on the cathode and shrinking on the anode. This swelling and shrinking results in the bending of the IPMC and shows a large dynamic deformation that can be controlled by the applying voltage. Usually, IPMC EAPs require only low voltages. IPMC devices can achieve more than 5% strain and large bending, but these actuators tend to be slow, due to the high relaxation times.

A typical device based on an IPMC consists of a polymer with ions and more than one electrode. Electrodes may be placed in opposite sides of the polymer or on the same side. Different orientations of the electrodes result in distinct deformation of the polymer. For example, Chang et al. designed an IPMC based actuator by placing both electrodes on the same side of the polymer, yielding an “S” shape when actuated.<sup>[128]</sup> A schematic comparison of two actuators that result from placing electrodes in different configurations is presented in Figures 4.<sup>[128]</sup> The left diagram (B) presents a device with two electrodes placed on opposite sides of the polymer while the right diagram (B) shows one device for which two electrodes are placed on the same side, with a conductive

layer positioned opposite. This resulted in different deformations of the IPMC and different shapes (Figure 4C, bottom). Several other examples of soft actuators,<sup>[129,130]</sup> tactile sensors,<sup>[131]</sup> and Braille displays<sup>[132,133]</sup> based on IPMCs have also been developed.

**Conductive Polymer Actuators:** Conductive polymers that are used in actuation are semiconducting materials which, when doped, become conductors. Similar to IPMCs, the conducting polymer actuators are also sandwiched between two electrodes, which are often intrinsically conductive polymers. However, unlike the IPMCs, the actuation mechanism of the conducting polymers is driven by electrochemical reduction or oxidation. When an electric potential is applied to the conductors, electrical charges are added or removed to the polymer which results in changes of ions in the polymer depending on the type of the dopant. This mass transport results in changes in the volume of the polymer. The change in volume depends on the doping of the polymer, their mobility, and on the applied electric field.

The operation principle for a conducting polymer based actuator is illustrated in Figure 4D.<sup>[134]</sup> In this example, the authors used conducting interpenetrating polymer networks (C-IPNs) that consisted of two electronic conducting polymers (ECPs) and within the electrodes a solid polymer electrolyte (SPE). The SPE was realized from poly(ethylene oxide) (PEO) and nitrile butadiene rubber (NBR) and acted as an ion reservoir. When a voltage (2 V) was applied to the electrodes, the SPE layer deformed or bent depending on the bias that generated or removed ions from the electrodes.

Conductive polymer actuators have the advantages of requiring low operating voltages, and supplying high tensile strength. More than 40% strain can be achieved using conductive polymers. However, a high current is required to operate conductive polymer actuators, which are limited by the mobility of the ions. These materials also have been used to demonstrate a variety of actuators.<sup>[47,135]</sup>

### 4.3. Electromagnetic Actuators (EMAs)

Electromagnetic actuators are based on basic principles of electromagnetism. Such actuators use electromagnetic forces to perform mechanical work. The electromagnetic force is described through Faraday's laws of electromagnetic induction, the Lorentz force law of forces, and the Biot-Savart law. Faraday's law relates the magnetic and electric fields, and predicts forces generated by electromagnetic induction. The Lorentz force law predicts forces acting on a charged particle moving in electric and magnetic fields. The Biot-Savart law describes the magnetic field produced by a stationary electric current. Typical EMA devices consist of an electrical circuit and a magnetic circuit, and the resulting magnetic force is proportional to the electric current. Several actuators have been developed based on these principles, including DC motors, AC motors, stepper motors, voice coil motors, and others. Variable reluctance actuators (VRAs), such as solenoids, operate on the principle of magnetic attraction of ferromagnetic materials.

A VRA is constructed from an inductor in proximity with a ferromagnetic material (solenoid or variable reluctance actuator). When a current is passed through the coil, the resulting magnetic field attracts the metal. While this method can produce large forces over a wide frequency range, the effect is always attractive and requires care to control.<sup>[136,137]</sup>

An EMA is constructed from an inductor in proximity to a permanent magnet. A typical arrangement is illustrated in Figure 5A.<sup>[138]</sup> A permanent magnet is suspended using an elastomer membrane centered over a planar coil. When an electrical current is passed through the coil, the permanent magnet is repelled or attracted by the induced magnetic field by the coil. If the magnetization of the permanent magnet is  $\mathbf{M}$ , then the total magnetic force  $\mathbf{F}$  is

$$\mathbf{F}_i = \int_V \frac{\partial}{\partial x_i} (\mathbf{M} \cdot \mathbf{B}) dV \quad (8)$$

where,  $\mathbf{B}$  is the external magnetic field induced by the coil and  $V$  is the volume of the permanent magnet.

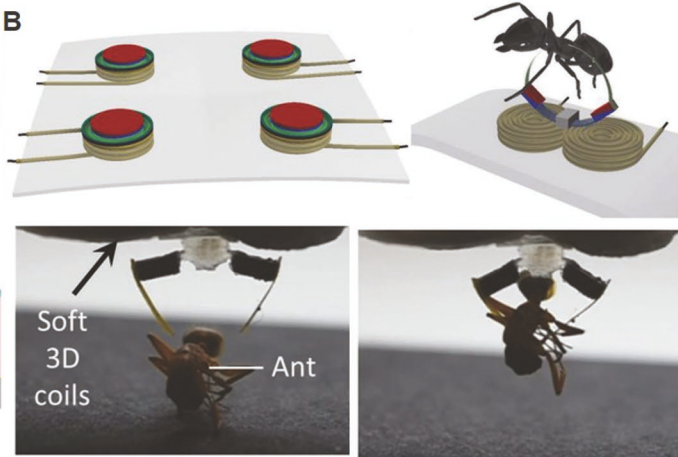
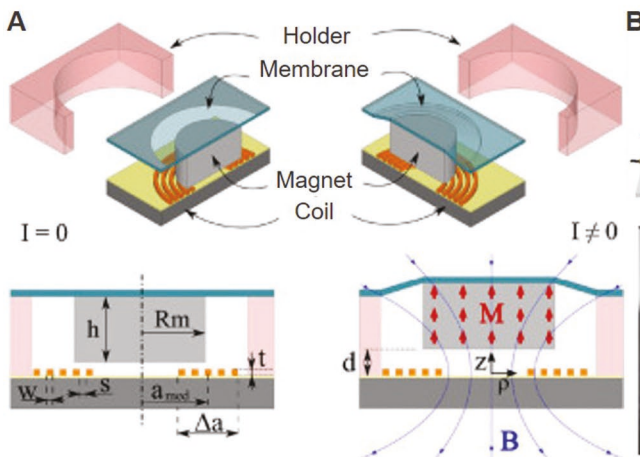


**Figure 5.** A) Schematic illustration of a magnetic system using a suspended permanent magnet and a coil. Reproduced with permission.<sup>[138]</sup> Copyright 2015, Elsevier B.V. B) Schematic illustration of an actuator based on electromagnetic principle (top) and the photographs of the EMA lifting small load (bottom). The coils are realized using eGaN. Reproduced with permission.<sup>[139]</sup> Copyright 2018, WILEY-VCH Verlag GmbH and Co. KGaA, Weinheim.

two types based on their polarization mechanisms. The first category is known as dielectric electrorheological (DER), where dispersed particles in a nonconducting fluid medium become electrically polarized while an electric field is applied. The other type comprises randomly oriented molecular dipoles which reorganize upon application of an electric field.<sup>[148]</sup> The latter results in what is termed as the giant electrorheological (GER) effect. Since this type of actuator uses a liquid phase that must be encapsulated, this becomes a design constraint. However, this type of actuator can generate high forces when appropriately designed.<sup>[149]</sup>

ERF actuators can be operated in three modes: squeeze, flow, and shear (Figure 6A–C).<sup>[150]</sup> Squeeze mode generates dynamic forces, but is constrained to small displacements. In this mode, the ERF is sandwiched between two conductors, one of which is separated by a mesh (Figure 6A). In flow mode, the fluid motion is controlled via electrostatic valves as shown in Figure 6B. In the shear mode, the electric field controls the ERF between two surfaces that can be moved against one another (Figure 6C). A large number of haptic devices<sup>[150–155]</sup> and tactile displays<sup>[156–158]</sup> have been realized using ERF.

ERF based actuators are highly useful where strong power is needed with high bandwidth. But, the breakdown voltage of the ERF is often very low. Additionally, liquid driving material makes the device physically complicated.

#### 4.4.2. Magnetorheological Fluid Actuators

Magnetorheological fluids are suspensions of free flowing ferromagnetic particles, such as iron, in a carrier fluid such as glycerin. An MRF changes viscosity upon applying electric field.<sup>[159,160]</sup> When a magnetic field is applied to the fluid, the ferromagnetic particles align along the applied flux lines,

yielding a change in viscosity. An MRF can exhibit yield stresses on the order of 50–100 kPa with a response time on the order of 1 ms.<sup>[161–163]</sup>

An example of an MRF based actuator (Figure 6D,E) was realized by Ishizuka and Miki, who mixed oxidized iron particles as magnetic particles with poly- $\alpha$ -olefin.<sup>[59]</sup> The average size of the iron particles was 2  $\mu\text{m}$ . The MRF was embedded in a composite rubber substrate. In the absence of any magnetic field, the particles were distributed uniformly in the base liquid and the MRF acted as a normal liquid (Figure 6D). When an external magnetic field was applied, the iron particles aligned with the magnetic field, greatly changing the stiffness of the MRF (Figure 6E). Several other demonstrations of haptic devices based on MRF actuators have been reported<sup>[59,60,164–167]</sup> including several tactile displays.<sup>[168–171]</sup>

MRF based actuators can produce very strong forces, but often require the driving material to be liquid, which can lead to cost and design constraints. In addition, these devices resist motion rather than producing motion.

#### 4.5. Liquid Crystal Actuators

Liquid crystals are a special state of some materials that comprise semiliquids with intrinsic crystal orientations. Due to their optical properties, such materials were first used for visual displays. These materials can also respond to external stimuli that evoke reversible mechanical changes. A wide range of polymeric liquid crystal has been synthesized<sup>[172,173]</sup> and many of these have been used for actuation.<sup>[174,175]</sup> The operating principle of these materials involves rapid phase transitions between nematic and isotropic phases. Normally, liquid crystal elastomers (LCEs) contain rigid, anisotropic mesogenic units incorporated within polymer chains that remain

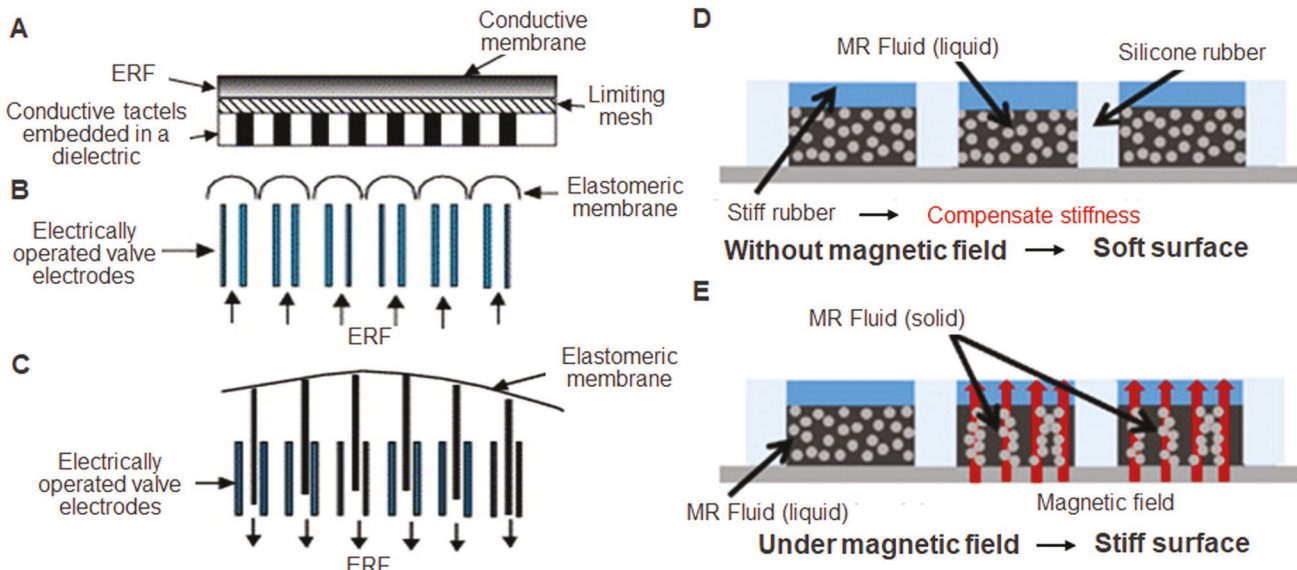


**Figure 6.** Different operation modes of ERF actuators: in squeeze mode A), in flow mode B), and in shear mode C). (A–C) Reproduced with permission.<sup>[150]</sup> Copyright 2005, Elsevier Ltd. D) Schematic working principle of MRF based actuators. Without any external magnetic field the suspension acts as a liquid which turns nearly to a solid under external magnetic field E). (D,E) Reproduced with permission.<sup>[59]</sup> Copyright 2017, The Japan Society of Applied Physics.

mobile. When stimulated to the nematic phase, the mesogenic units become aligned in a direction without any crystalline orientation. The phase transformation can be created in response to thermal excitation, ultraviolet excitation, or electrical stimulation.<sup>[176–178]</sup>

A number of LCE based actuators have been demonstrated for different applications including refreshable Braille displays,<sup>[61,62]</sup> tactile sensors,<sup>[173]</sup> or soft robotics.<sup>[38,179]</sup> As one example, Rogóz et al. developed a soft robot based on LCE that could mimic caterpillar locomotion. The robot was realized using a mixture that contained a liquid crystal monomer, liquid crystal crosslinker, and green light absorbing dye.<sup>[38]</sup> When polymerized in the nematic phase, the polymer could contract 18% in parallel and expand 10% in the perpendicular direction to the molecular orientation, which was reversible. Thermal stimulation was used to reversibly change the phase of the liquid crystal elastomer.

#### 4.6. Gel Actuators

There are several gels that can convert chemical energy to mechanical energy when stimulated.<sup>[180]</sup> For example, when poly(acrylic acid) (PAA) is cross linked with glycerin or poly(vinyl alcohol) (PVA), esterification occurs which results in mechanical energy exchange.<sup>[181]</sup> The basic principle of this actuation mechanism is that the pH changes in the polymers, ionizing the polyelectrolyte. There are also salt-responsive gels, such as collagen fibers, which, when mixed with LiBr, KSCN, or urea, can generate mechanical energy due to the chemical melting and crystallization of the polymers.<sup>[182]</sup> On the other hand, thermoresponsive gels are sensitive to temperature changes. There are many polymers, including natural polymers, that change viscosity and volume when a change in temperature occurs. However, most practical actuators based on thermoresponsive gels combine natural and synthetic polymers to modify thermal response properties.<sup>[183,184]</sup>

There are many other gels that exhibit mechanical deformations based on a variety of designs. Many of those have been used to realize actuators.<sup>[46]</sup> For example, solvent-responsive gels,<sup>[185]</sup> photoresponsive gels,<sup>[39,186]</sup> magnetoresponsive gels,<sup>[187]</sup> and electroresponsive gels<sup>[188]</sup> have been used for actuator design. There are also several examples of tactile displays using gels.<sup>[63,64]</sup> A wide range of gels are available that can be stimulated in different manners that lend themselves to robust effects. However, the gels must be maintained in semiliquid form which can make the resulting devices mechanically sensitive. Additionally, the gel actuators typically result in relatively low bandwidths.

#### 4.7. MEMS Actuators

While often relying on conventional rigid materials, microelectromechanical system or MEMS based devices comprise highly integrated miniature mechanical and electrical components, often realized using microfabrication techniques. MEMS actuators generate motion from energy through

physical or mechanical energy conversion. The underlying actuation mechanism can be any of the methods discussed earlier, such as can be integrated within microscale devices.<sup>[189]</sup> Since the physical dimensions of such a device are in the micrometer range, small spatial dimensions can be achieved. Also, bandwidths are possible. However, the manufacturing methods required are complicated and difficult to scale. A number of demonstrators of emerging haptic devices based on MEMS methods have been realized, including tactile displays and sensors.<sup>[190–195]</sup>

#### 4.8. Other Actuator Technologies

Several other actuator mechanisms have been widely used for haptic devices but are omitted here, since they rely on more conventional materials and methods. For example, shape memory alloys (SMA) comprise phase changing metal alloys whose mechanical state can be reversibly switched depending on the temperature changes.<sup>[196,197]</sup> There are also examples of nylon based actuators,<sup>[198,199]</sup> including commercial nylon fishing line, which can be used to realize lightweight thermally switched actuators. These actuators can provide high power with low hysteresis, and can be designed to function over a wide range of temperatures. Other phase change material properties have also been used to actuate tactile devices. Shikida et al. demonstrated a tactile display based on liquid–vapor phase change which was used to drive the actuators.<sup>[200]</sup> The device comprised of  $3 \times 3$  array of actuators and each actuator had a needle, a heater, and a driving liquid sealed in a cavity. A change in phase of the liquid to vapor increases the volume which is used to generate the stroke at the actuators. Other actuators include thermally mediated polymer actuators,<sup>[201]</sup> chemically mediated actuators,<sup>[202,203]</sup> and optically mediated actuators.<sup>[204,205]</sup> The thermal nature of such processes constrains the feasible operating speed and bandwidth.

#### 4.9. Summary: Emerging Actuation Methods for Tactile Feedback

A wide range of actuation methods are described in the literature. Frequently, functional devices require the combination of multiple such mechanisms or design elements. The choice of actuation mechanism to realize a functional device is determined by the application requirements and materials involved. Table 2 summarizes an array of actuation mechanisms used in tactile displays.

### 5. Fabrication Methods for Emerging Materials

Fabrication processes play key roles in the realization of functional devices, especially in manufacturing. However, the choice of fabrication method is closely related to the materials involved. Flexible and soft materials are not commonly involved in the fabrication of many conventional mechanical or electrical devices, or manufacturing methods. Thus, the integrated processing of

**Table 2.** Summary of emerging material actuation methods for tactile displays.

Transduction technique	Mechanism	Advantages	Disadvantages
Pneumatic	Compressed air	Simple, lightweight, high power-to-weight ratio	Low bandwidth, stiff
Hydraulic	Compressed liquid	High bandwidth, high power	Bulky and heavy
Electronic EAP	Electric field driven	Fast, high actuation force, high mechanical energy density, long lifetime	High operating voltage
Ionic EAP	Ionic diffusion	Voltage control bidirectional, low operating voltage	Liquid electrolyte, slow response, low actuation force
Piezoelectric	Piezoelectric effect	Small dimension, large force, high resolution frequency, fast, low power consumption	Small motion, high driving voltage
Electrovibration	Coulomb force	Fast, low-powered, dynamic	Relatively high noise
Electromagnetic	Electromagnetism	Wide bandwidth	Heat generation
ERF	Change in viscosity by electric field	Very fast, high power	Liquid suspension, low breakdown voltage
MRF	Change in viscosity by magnetic field	Strong force	Liquid suspension, expensive
LCE	Phase transition	Wide bandwidth, well controlled	Liquid medium
Gel	Chemical reaction	Different stimulus, well controlled	Relatively low bandwidth, semiliquid medium
MEMS	Electromechanical	Miniature, wide range bandwidth	High-tech fabrication, rarely soft

these materials is less standard in the actuator industry, and a variety of fabrication techniques are proposed in the literature, most of which are not yet brought to large-scale industrial manufacturing. The experimental nature of many of the devices reviewed here means that less attention has been given to the reliability and robustness of manufacturing processes.

Fabrication requires that the materials to be used, the requirements for the device, including resolution and size, be taken into account. If a device requires resolution in the microscale over a large area, a microprinting method might be preferred to a 3D lithography method. On the other hand, microprinting methods are not compatible with all materials. Next generation tactile display devices will require high resolution fabrication over large areas, and may demand the use of flexible or soft substrates, which can be conformal. In the following section we review several relevant technologies, but a comprehensive account of the continuously growing array of fabrication methods that could be used for such devices would be beyond the scope of this article.

### 5.1. Microfabrication

Microfabrication processes are typically used to fabricate devices that require micro or nanoscale detail, which cannot be readily achieved via machining. Such technologies are mature, and have been widely used in modern devices that require high resolution features, including processes that produce many devices we use in daily life.

The manufacturing of a device using microfabrication methods involves a number of variable processing steps. To give an example, the fabrication of a micro-electromechanical system might require a number of patterning steps to define a device layer and electrodes. The steps may involve lithography processes, in which a resist mask is used to pattern an electrode layer. Advanced lithography processes, used in IC manufacturing, can realize patterns with resolutions on the order of 10 nm. Typically, electrodes are deposited via a metallization

process such as sputtering or evaporation which can deposit a material layer from a few angstroms to a few micrometers in thickness. The electrode material is deposited as a continuous thin film which is patterned using a method called lift-off using a lithography method. A reverse method can also be used, where the electrode material is deposited prior to a lithography step, in combination with a subsequent etching process that defines the electrodes.

A complex device might require a large number of complex processing steps. For example, a MEMS device might also require a doping step, where the bulk substrate is precisely doped with a carrier (yielding holes or electrons) to modify the mobility or type of the substrate. This process often requires high temperatures, approaching 1000 °C. Such processes also often require the device layer to be released from a bulk substrate in order to make them thin and flexible. A common approach for realizing thin device layers is to use a silicon-on-insulator (SOI) substrate, where a thin active device layer is bonded with a carrier wafer via a sacrificial insulator layer. When the entire device is fabricated on the active layer, the insulator layer is then chemically removed, yielding a free-floating active device layer.

Future tactile display devices will require high resolutions, for which microfabrication methods are particularly useful. However, these techniques are constrained to special materials and are largely incompatible with soft or fluidic substrates, unless the processes are greatly modified. Typically, most MEMS electromechanical devices use at least a few microfabrication processes. Many tactile display devices have been developed based on microfabrication techniques.<sup>[206–208]</sup>

### 5.2. Soft Lithography and Molding

Soft lithography and molding processes are extremely useful when large area patterning is required with microscale resolution on a compliant substrate. In general, soft lithography processes involve a “master,” on which the negative patterns are

realized, and an elastomer that is cast and cured on this master to replicate the patterns. After curing, the elastomer replica is removed from the master, producing the desired patterns. The master can be produced using conventional microfabrication methods, and can be used several times for replication. Versions of this method were used to contact print self-assembled monolayer (SAM) structures on a target substrate that could guide subsequent material deposition onto the substrate.

There are many examples of haptic devices using soft lithography and molding techniques.<sup>[102,133,209–212]</sup> For example, Son et al. demonstrated a flexible tactile display based on molding technique using PDMS.<sup>[211]</sup> They formed a number of pneumatic microchannels in a PDMS layer. An SU-8 layer was used to form the master via photolithography. Other actuation mechanisms such as EAP,<sup>[102,133]</sup> electrostatic,<sup>[137,213–215]</sup> and electromagnetic<sup>[208,216]</sup> have also employed soft lithography and molding techniques.

### 5.3. Additive Manufacturing

Additive manufacturing methods have been widely appreciated for their ability to realize 3D functional devices via a unified process. Typically the term refers to methods where 3D structures are manufactured layer by layer without the removal of materials. A number of methods based on this principle have been introduced recently, including 3D layer printing, inkjet printing, laser printing, selective laser sintering (SLS), fused deposition modeling, and stereolithography. Each of these methods has advantages and drawbacks. Most are tailored to particular material types, and all have characteristic resolution limits.<sup>[217]</sup> Here, we discuss a few of these methods.

#### 5.3.1. 3D Printing

3D printing is an emerging technology with potential applications in the field of electromechanical devices. In general, the method forces solid or liquid materials (“inks”) through a nozzle to construct a 3D structure. More advanced 3D printers can print inside a liquid bath by optically curing a material.<sup>[37]</sup> The mechanical property of the final device depends on the ink. Since 3D printers use a computer aided 3D design to manufacture the object, the design of the object comprises any shape, within support limitations. However, the minimum feature sizes, and minimum surface roughnesses, that can be achieved are limiting factors. There are several examples of actuators<sup>[218,219]</sup> and haptic devices<sup>[220,221]</sup> that have used 3D printers. For example, Martinez et al. realized haptic devices for educational applications based on 3D printing methods.

#### 5.3.2. 2D Printing

2D printing technologies are extremely useful for large-area device manufacturing, due to their scalability and low cost. A variety of printing methods are used in device fabrication. Examples include screen printing, inkjet printing, and gravure. In screen printing, a mesh is used to pattern substrates,

via patterns that are formed using liquid inks. The resolution of such methods is limited by the mesh. It is challenging to realize multilayer, complex devices using this method. Consequently, it is most widely used for simple devices, such as flexible and wearable devices.<sup>[53,222,223]</sup> Yun et al. fabricated a cellulose based electroactive paper for haptic applications using screen printing methods.<sup>[53]</sup> They bonded 28 µm thick EAPap with a thin, metallic membrane using a conductive ink. The conductive ink comprised silver paste screen printed onto the surface of the metallic film. In another approach, Pyo et al. screen printed a CNT-PDMS layer on a microfabricated Si/SiO<sub>2</sub>/Au substrate.<sup>[222]</sup>

Inkjet printing uses a liquid ink propelled through a nozzle using capillary methods. The force impelling the ink characterizes the type of printer. Piezo inkjet printers use mechanical impulses to generate precise ink droplets. Thermal inkjet printers rely on heating to generate droplets for deposition. Other inkjet processes include those employing electrostatic charges or acoustic waves. Several haptic devices have been realized using inkjet printing methods.<sup>[223–225]</sup>

The minimum feature size that can be achieved using screen or inkjet printing method is 20 µm. The layer thickness in such a process can be less than a 100 nm. Screen printing methods are fast, low cost, and parallelizable. In contrast, inkjet methods are relatively slower. Using the latter, it is also more difficult to realize thick layers.

#### 5.3.3. Laser Based Processing

These fabrication methods include selective laser melting (SLM), selective laser sintering, stereolithography, and two-photon direct laser writing. In essence, such methods employ a laser source to solidify, melt, or activate material layers. The modified base materials can comprise powders, liquids, or photosensitive resins. An example of the application of laser sintering methods for the manufacture of haptic devices was reported by Price and Sup IV.<sup>[226]</sup> They developed a handheld haptic robotic device incorporating a selectively laser sintered nylon powder structure.

### 5.4. Transfer Printing

The transfer printing method uses a donor substrate to fabricate the active regions of devices for later transfer to the final substrate. Since this method uses an external carrier substrate, which can be rigid, to realize the active devices, it is able to fabricate comparatively complex devices. However, this method can be slow and involve complexities when the active devices are very small, and may further involve multistep transferring. There are several examples of the use of transfer printing methods for realizing haptic devices.<sup>[227,228]</sup> Ju et al. realized a tactile feedback touch screen based on transfer printing methods.<sup>[227]</sup> They used a glass substrate first to screen print a uniform layer of poly(vinylidene fluoride-trifluoroethylene-chlorotrifluoroethylene) [P(VDF-TrFE-CTFE)] and later to laminate it with another layer of elastomer. Then they transferred the [P(VDF-TrFE-CTFE)] and the support elastomer

**Table 3.** Fabrication techniques summary.

Methods	Minimum resolution	Advantages	Disadvantages
Microfabrication	A few nm	Highly developed, well controlled, high resolution	Costly, typically not compatible for soft materials
Soft lithography	A few hundred nm	3D structures, parallel processing, cheap	Only compatible with soft materials
Molding	A few hundred nm	Large area processing, easy, cheap	Depends on the master, only compatible with soft materials
3D printing	>0.1 mm	3D structure, wide range of designs	Low resolution, slow, expensive, limited materials choice
Screen printing	>20 $\mu$ m	Parallel processing, cheap	Low resolution, limited materials choice, limited geometry
Inkjet printing	>20 $\mu$ m	Fast, cheap	Low resolution, limited materials choice
Laser processing	A few hundred nm	Fast, wide range of designs	Expensive, limited materials choice
Transfer printing	<1 $\mu$ m	Robust, combines different methods, wide range of materials	Challenging for multilayer device

film by diffusing water through an interface of glass with [P(VDF-TrFE-CTFE)].

Though there are different technologies that are capable of realizing integrated active devices, most demonstrated devices use combinations of these techniques. This is because there is no single method that is compatible with all materials, and capable of manufacturing all kinds of device. The choice of technology largely depends on the materials and the requirements for the device. **Table 3** summarizes the fabrication methods reviewed here, along with their advantages and disadvantages.

## 6. Tactile Displays Based on Emerging Materials

There is a growing interest for using emerging materials to realize tactile display devices, based on two principal motivations. The first is the difficulty of realizing such devices using conventional technologies. The second is that such materials can afford new capabilities, ranging from electronic functions to greatly enhanced mechanical compliance or flexibility. For example, a common material used in conventional devices, silicon, has a Young's modulus greater than 100 GPa. In contrast, common silicone (PDMS) materials have Young's moduli lower than about 1 MPa, overlapping the range for human skin.<sup>[10]</sup> The comfort, conformability, and ergonomic advantages that such materials afford have attracted interest for applications in healthcare, wearable computing, and, increasingly, haptics.

### 6.1. Fluidic Displays

Among the most widely investigated technologies for tactile display are pneumatic systems, based on the fluidic actuation principles discussed in the foregoing. They have been widely used for soft haptic devices.<sup>[74–77]</sup> For example, Sonar and Paik demonstrated a soft pneumatic actuator (SPA) skin based on soft silicone.<sup>[74]</sup> In this multilayer device, they used a silicone–polypropylene–silicone stack where the polypropylene masking layer was used to pass air, resulting in inflation to a desired shape. In an another example, Wu et al. demonstrated a Braille display based on pneumatic actuation.<sup>[209]</sup> They used six endoskeletal microbubble actuators arranged in a 2  $\times$  3 array as Braille cells. The system consisted of three compartments including a pneumatic actuator layer which was operated under compressed air through valves. **Figure 7A** illustrates

the resulting Braille dots corresponding to Braille alphabets. The spatial resolution of the demonstrated tactile display was 2–2.5 mm, and the deflection of each Braille dot was nearly 0.6 mm at 100 kPa.

Another fluidic elastomeric actuator, which also integrated soft sensors, was developed by Robinson et al. for tactile machines.<sup>[229]</sup> This device employed two viscoelastic fluids for capacitive sensing of low mechanical stress and large strains. Feedback was provided by a soft, pneumatically powered display. **Figure 7B** shows an image and schematic of the multi-layer sensory and actuator system. To realize the actuator, the group used soft lithography on a silicone substrate. Input to each capacitive sensor resulted in a response via individual chambers due to pneumatic actuation. Other examples of smart tactile displays based on pneumatic principle are discussed.<sup>[76,209]</sup>

### 6.2. Electrostatic Tactile Displays

Several different electrostatic actuation methods have been explored, some of which have been applied to the design of tactile displays.

#### 6.2.1. An Electrostatic Mid-Air Tactile Display

Kamigaki et al. demonstrated a flexible and thin ultrasound tactile display based on electrostatic actuation of an array of membrane electrodes.<sup>[230]</sup> Each element of the device had three conductive layers, the top layer focuses on ultrasound in mid-air as a result of applied voltages to the constituent electrode-membranes. The nonlinear ultrasound acoustic signals yield an acoustic radiation force at tactile frequencies. To fabricate the devices, the authors used 100  $\mu$ m thick adhesive as a substrate, 12.5  $\mu$ m gold layers as an electrode, and a stainless-steel frame. The dimensions of the final device were 1 cm  $\times$  1 cm per emitter, across an 8  $\times$  8 array of emitters, and thickness 0.6 mm.

#### 6.2.2. Electrovibration Displays

In these devices, mechanical vibration is induced by an electrostatic force on a surface. In one example, Ilkhani et al.

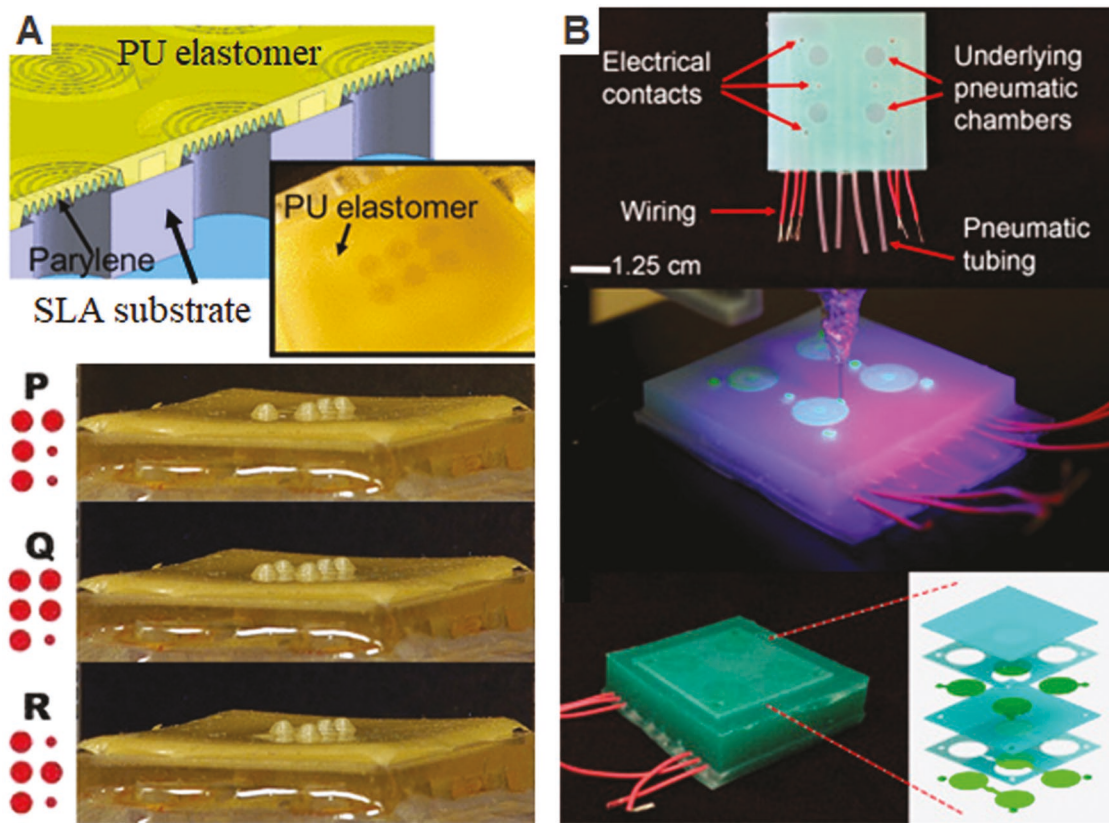


**Figure 7.** Pneumatic tactile displays. A) Schematic (top) and photographs of a pneumatic soft tactile display demonstrating different Braille alphabets (bottom) P, Q, and R. Reproduced with permission.<sup>[209]</sup> Copyright 2012, IEEE. B) Photographs and schematic of a pneumatic haptic display showing electrical contacts and pneumatic channels (top). Printing method of the device (middle) and the final device with schematic layer stacks (bottom). Reproduced with permission.<sup>[229]</sup> Copyright 2005, Elsevier Ltd.

presented a multitouch haptic feedback device<sup>[231]</sup> for which they realized a display with  $17 \times 17$  electrodes. When a high voltage AC signal was applied to pairs of nearby electrodes, a user could perceive changes in friction at the corresponding intersection. **Figure 8A** shows a photograph of the final device. The group used conventional microfabrication techniques to realize the device using aluminum as electrodes and Parylene-C as insulator.

A recent example of a flexible tactile display based on electro-vibration was reported by Ishizuka et al.<sup>[110]</sup> The authors used a thin layer of PEDOT/PSS as a conductor and PDMS as the substrate and as an insulating layer. The device was thin (total 70  $\mu\text{m}$  thick), transparent (Figure 8B), and flexible (Figure 8C). The PEDOT/PSS layer was sandwiched in between two PDMS layers; when there were no electric field, the rubbing finger on the surface felt no additional force.

#### 6.2.3. Electrotactile Displays

Electrotactile stimulation displays involve transmission of electrical charges through the skin for direct stimulation of the sensory nervous system. Tezuka et al. presented an electrotactile display that comprised a microneedle electrode array placed on the fingertip and a flat electrode placed on

the finger nail.<sup>[232]</sup> Stimulated current could flow from the microneedle to the flat electrode, which acted as a ground electrode as shown in Figure 8D. The needles were long enough to penetrate through the stratum corneum which reduced the operating voltage of the device. The group used Ti wires as the needle and PDMS as the base substrate. Figure 8E shows photographs of the tactile display and the needle array (left) with schematic stimulation flow of the needles (right).

#### 6.3. Dielectric Polymer Based Tactile Displays

There are a number of dielectric materials available including inorganic and organic materials that vary in dielectric properties. Patterning these devices with soft lithography or other methods makes it possible to create integrated arrays for tactile displays. In one example, Kim et al. created a transparent, stretchable tactile display based on graphene electrodes and dielectric polymer.<sup>[50]</sup> The demonstrated device was optically transparent and could sustain up to 30% strain with modest performance degradation.

In another example Phung et al. used dielectric elastomer actuator (DEA) to realize a tactile display that could produce a displacement of 350–140  $\mu\text{m}$  at 0.3–10 Hz.<sup>[233]</sup> Their

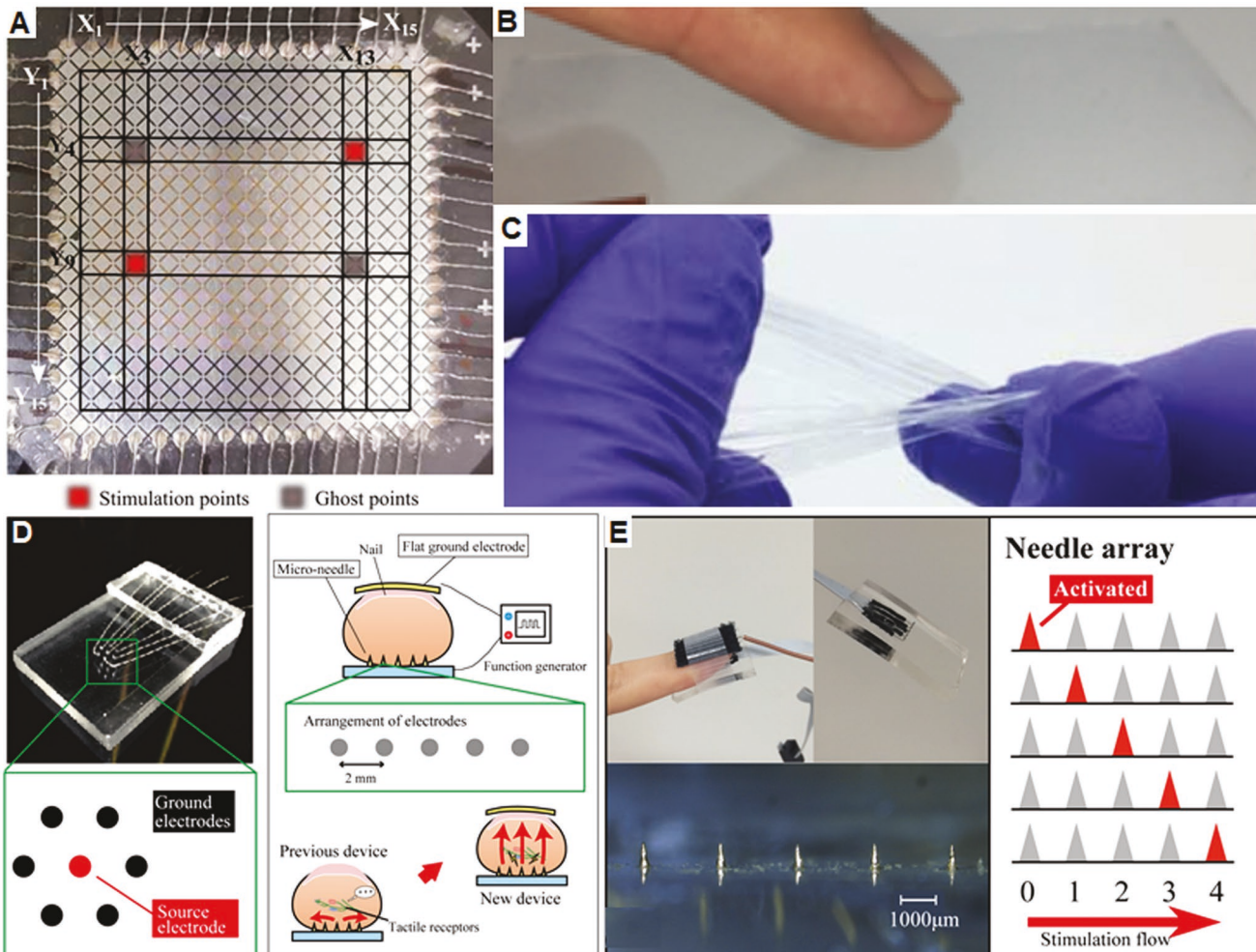


**Figure 8.** Electrostatic tactile displays. A) Photograph of a tactile display with multitouch feedback system based on electrostatic stimulation showing  $17 \times 17$  electrodes array. Reproduced with permission.<sup>[231]</sup> Copyright 2018, IEEE. B) Photograph of the flexible tactile display using thin PEDOT/PSS and PDMS layers, and C) photograph showing the flexibility of the device. B,C) Reproduced with permission.<sup>[110]</sup> Copyright 2018, the authors, published MDPI, Basel, Switzerland. Electrotactile display based on microneedles. D) Photograph and schematic design principle of the tactile display and E) photograph demonstrating flexibility of the device as can be worn on the finger (left) and schematic stimulation flow (right). D,E) Reproduced under Creative Commons Attribution License (CC BY 4.0).<sup>[232]</sup> Copyright 2016, the authors.

device consisted of a frame with a rigid coupling and a film type DEA as shown in **Figure 9A**. When no bias is applied to the device, the actuator remains under pretension due to the rigid coupling and actuators contract when a bias is applied and the rigid coupling moves down. The group used silicone molding process to fabricate the device frame and stacked layers of silicone and electrodes for the actuators. Figure 9A (bottom) shows a photograph of the device under operation. The same group used this method to demonstrate a flexible and wearable tactile display that could operate over a frequency range of 0–150 Hz and could generate a force of 50 mN.<sup>[43]</sup> The final device had  $8 \times 12$  tactile stimulator array that could be controlled individually (Figure 9B). The device was also integrated with tactile sensors. Marette et al. implemented a device comprised of zinc–tin oxide electrodes.<sup>[234]</sup> A voltage of 1 kV is applied across the dielectric in order to control the actuation of 16 independent actuators for a tactile display.

#### 6.3.1. Transparent Displays

For many mobile applications, the active area is expected to be transparent. Tiwari et al. demonstrated a transparent and flexible device for tactile feedback that could form local topographic features using a DEAP design.<sup>[51]</sup> The materials used were conductive hydrogel, silver nanowire (AgNWs), and conductive polymers, with acrylic as a dielectric layer. Figure 9C (top) shows the schematic cross-sectional view of the materials stack used to realize the tactile device. They used spray patterned AgNWs for the top electrodes and acrylamide-sodium chloride conductive hydrogel for the bottom electrodes. The transparency of their device is demonstrated in Figure 9C. The flexibility of this device was judged to be initially insufficient for wearable applications. This issue could be resolved using an elastomer as a base substrate. Koo et al. realized a wearable tactile display based on a soft actuator, using an EAP.<sup>[235]</sup> In their design they used a thin circular incompressible elastomer film which was

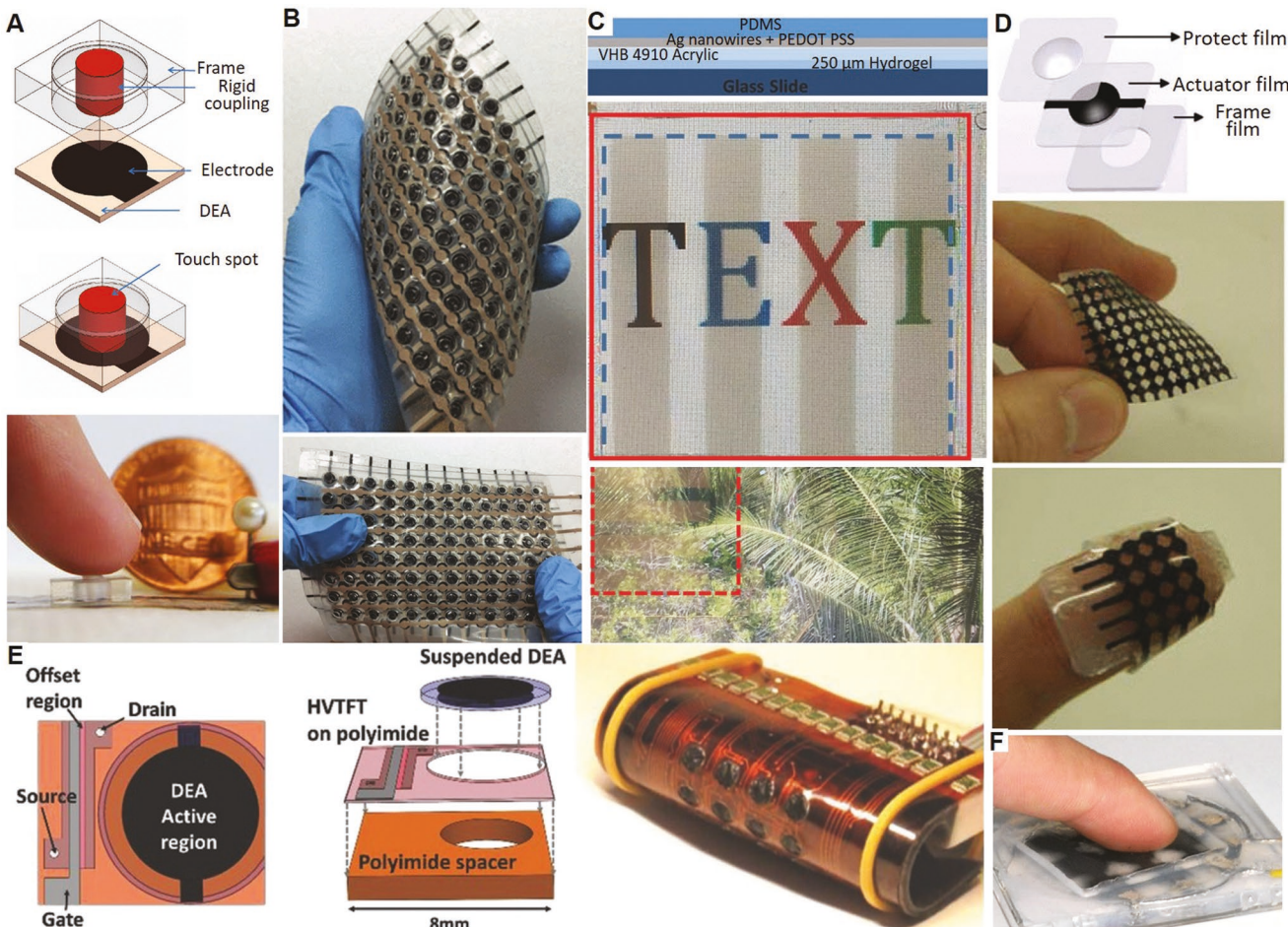


**Figure 9.** Dielectric elastomer actuator based tactile displays. A) Schematic design principle and assembled device (top), and photograph of the tactile display under operation showing the relative dimension (bottom). Reproduced with permission.<sup>[233]</sup> Copyright 2015, Springer Science+Business Media Dordrecht. B) Interactive flexible and stretchable tactile display with integrated tactile sensors. Each stimulator of the  $8 \times 12$  array could be stimulated individually. Reproduced with permission.<sup>[43]</sup> Copyright 2017, IEEE. C) Schematic cross-sectional view of the stack layers of the device (top) and photographs of the display showing the transparency of the device (middle and bottom). Reproduced with permission.<sup>[51]</sup> Copyright 2017, WILEY-VCH Verlag GmbH and Co. KGaA, Weinheim. D) Schematic illustration of device layers and actuation mechanism (top) and photograph demonstrating flexible (middle) and wearable (bottom) tactile display. Reproduced with permission.<sup>[235]</sup> Copyright 2008, IEEE. E) Schematic top (left) and tilted view (middle) of a single taxel of a flexible DEA based tactile display showing the integrated transistor and DEA active region. Photograph of the haptic display with  $4 \times 4$  taxel array showing a bending curvature of 5 mm (right). Reproduced with permission.<sup>[234]</sup> Copyright 2017, WILEY-VCH Verlag GmbH and Co. KGaA, Weinheim. F) Photograph of a  $3 \times 3$  tactile matrix realized using multilayer DEAs. Reproduced with permission.<sup>[98]</sup> Copyright 2009, IEEE.

attached inside a rigid cylindrical boundary frame. The elastomer deforms when a voltage is applied and forms a concave or convex shape as shown schematically in Figure 9D. For the electrodes, the group used spray coated carbon powder solution through a patterned mask onto the elastomer. To reduce the driving voltage, a multilayer stack of the dielectric elastomer was used which resulted in a total thickness of 210  $\mu\text{m}$ . The authors demonstrated flexible and wearable tactile display (Figure 9D) with  $4 \times 5$  tactile cells. The device could fit on the distal part of a human finger (Figure 9D, bottom).

### 6.3.2. Wearable Displays

There is a growing interest in wearable electronic devices, including haptic devices. Conformal contact of devices with the skin can be beneficial in such devices, aiding the consistency of

tactile stimulation. In addition to the aforementioned example (see Figure 9D), one wearable tactile device was demonstrated by Frediani et al., based on dielectric elastomer actuators,<sup>[236]</sup> for applications in virtual reality. The device was wireless and lightweight, and designed to wear on the fingertip. The group used a hydrostatically coupled dielectric elastomer. An incompressible fluid of spherical shape was encapsulated between two elastomeric membranes, one of which was a dielectric film and other of which was an electromechanically passive membrane. The dielectric active membrane, which was coated with electrodes, expanded upon applying an electric field to the electrodes, which caused the passive membrane to deflect inward, stimulating the fingertip. The membranes and the electrodes were fabricated using acrylic elastomer and carbon grease, respectively. Further motivation for realizing new skin-worn devices has motivated a variety of developments and applications.<sup>[43,69,222,223,235,237,238]</sup>

### 6.3.3. Reduced Voltage DEA Based Displays

As mentioned earlier, dielectric actuators usually require high voltages, in the range of several kV. This makes the method challenging to integrate with other electronic components. Marette et al. demonstrated a zinc–tin oxide based transistors integrated with a DEA based haptic display (Figure 9E). The final device consisted of a  $4 \times 4$  taxel array in active matrix fashion in which each taxel can be addressed individually. Figure 9E shows the device design with integrated transistor and DEA active region for a single taxel. The DEA had a PDMS membrane fabricated using a casting method. The electrodes were transferred to both sides of the membrane. As shown in the figure, each DEA consisted of a 4 mm diameter membrane and 17  $\mu\text{m}$  thickness electrodes, facilitating the use of moderate voltages. The DEA was interfaced with a transistor's source, drain, and gate terminals using a  $\text{CO}_2$  laser. The device remained highly compliant.

Another example was reported by Matysek et al. (see Figure 9F).<sup>[98]</sup> In their device, the authors used a multilayer stack of DEA materials and electrodes arranged in a checkerboard manner. As a dielectric material, they used 10  $\mu\text{m}$  thick PDMS and 2  $\mu\text{m}$  thick graphite powder layers as electrodes, which was electrodeposited using a shadow mask. The electrodes were locally overlapped in different layers yielding active regions those would deform when an electric field was applied to the electrodes.

The performance of actuators based on dielectric materials depends on the dielectric properties of the material. However, this property can be modulated over a wide range of values through the addition of conducting particles. For example, Park et al.<sup>[97]</sup> used plasticized poly(vinyl chloride) (PVC) gel to demonstrate vibrotactile actuators. They mixed  $\text{SiO}_2$  nanoparticles with the PVC gel (ePVC) to increase the dielectric property of the ePVC. The device consisted of three layers. Upper and lower layers had the electrodes and the middle layer was a wave-shaped ePVC gel. When an electric field is applied, the ePVC is deformed toward the anode. The state was rapidly reversible by removing the electric field.

### 6.4. Electromagnetic Tactile Displays

Electromagnetic actuation serves the majority of motion control needs in existing devices and systems, and can achieve high bandwidths and dynamic ranges such as are needed in many tactile display applications. Zarate et al. developed a tactile display based on electromagnetic actuators using two soft elastomeric membranes.<sup>[145]</sup> Figure 10A shows an image of their device (top). It consisted of  $4 \times 4$  array of vertical actuators. Each EMA consisted of a permanent magnet partially embedded in a soft magnetic material that was suspended between two elastomer membranes. These parts were placed over planar coils and were supported by an acrylic holder. When current is applied to the coil, a force is exerted on the permanent magnet. The bottom figures (Figure 10A) illustrate the operation of the tactile display, by demonstrating six different states of the actuators that correspond to different symbols. Each actuator could be displaced up to 0.55 mm exerting 40 mN force using

1.7 W power. Although this device used elastomers to position the magnet, the device was attached to a rigid surface, which rendered it effectively rigid. A flexible tactile device was demonstrated by Gallo et al. It integrated a thermal (Peltier) element, heatsink, and temperature sensor.<sup>[212]</sup> Figure 10B shows the device design (top) and operation (bottom). The group used a flexible printed circuit board (FPCB) and PDMS as base materials. As presented schematically, each taxel of the display comprised a permanent magnet, a coil, a core, a Peltier element, and a heatsink. The permanent magnet was attached to the thin PDMS membrane and aligned to the coil and to the core. In normal conditions, the permanent magnet was latched to the core. When a current was applied to the coil, the generated magnetic force repelled the permanent magnet that deformed the membrane. The final device comprised a  $2 \times 2$  array, each element of which could operate independently (Figure 10B, bottom).

In another example, Son et al. developed a multimodal flexible tactile display for teleoperation applications.<sup>[211]</sup> A combination of pneumatic and electromagnetic forces was used to actuate the display. To enable tight contact to any curved surface, they used a 100  $\mu\text{m}$  thick PDMS layer as a base material, yielding flexibility. Four permanent magnets with 2 coils were integrated in the layer. The fabrication process involved PDMS molding and microfabrication. The final device consisted of a  $4 \times 1$  array of tactile display. The device could generate about 200 mN force and nearly 1 mm displacement while applying 300 mA pulse current for 5 ms. There are numerous examples of haptic devices based on electromagnetic actuators, including a number that have been developed from emerging materials, for applications in automotive cockpits,<sup>[144]</sup> mobile internet,<sup>[239]</sup> and information display.<sup>[240,241]</sup>

### 6.5. Liquid Crystal Elastomeric Tactile Displays

Liquid crystal elastomers are particularly amenable to applications for tactile displays, since they can be easily rendered refreshable. At the same time the devices can be soft, light, and portable.<sup>[61,62]</sup> As discussed earlier, the stimulation of LCE can be performed in different manners. For example, Camargo et al. proposed a refreshable tactile display that could be optically actuated.<sup>[61]</sup> They used CNTs embedded in a LCE matrix (LCE-CNTs) that could reversibly change shape upon stimulation by light. The device contained a rigid skeleton (mold) and a thin layer of LCE-CNTs. The specific geometry of the LCE-CNTs was formed through a punch and die method. When the LCE-CNT film was stimulated by light, the film expanded and deformed locally since the rigid skeleton mechanically supported the film elsewhere. However, their device possessed a relatively longer recovery time (6 s), which might be considered as a drawback of the system. A similar method was used by Torras et al. to realize another tactile display.<sup>[62]</sup>

### 6.6. Composite Material Displays

Although there are often several possible tactile display devices that can be formed from any of the actuation

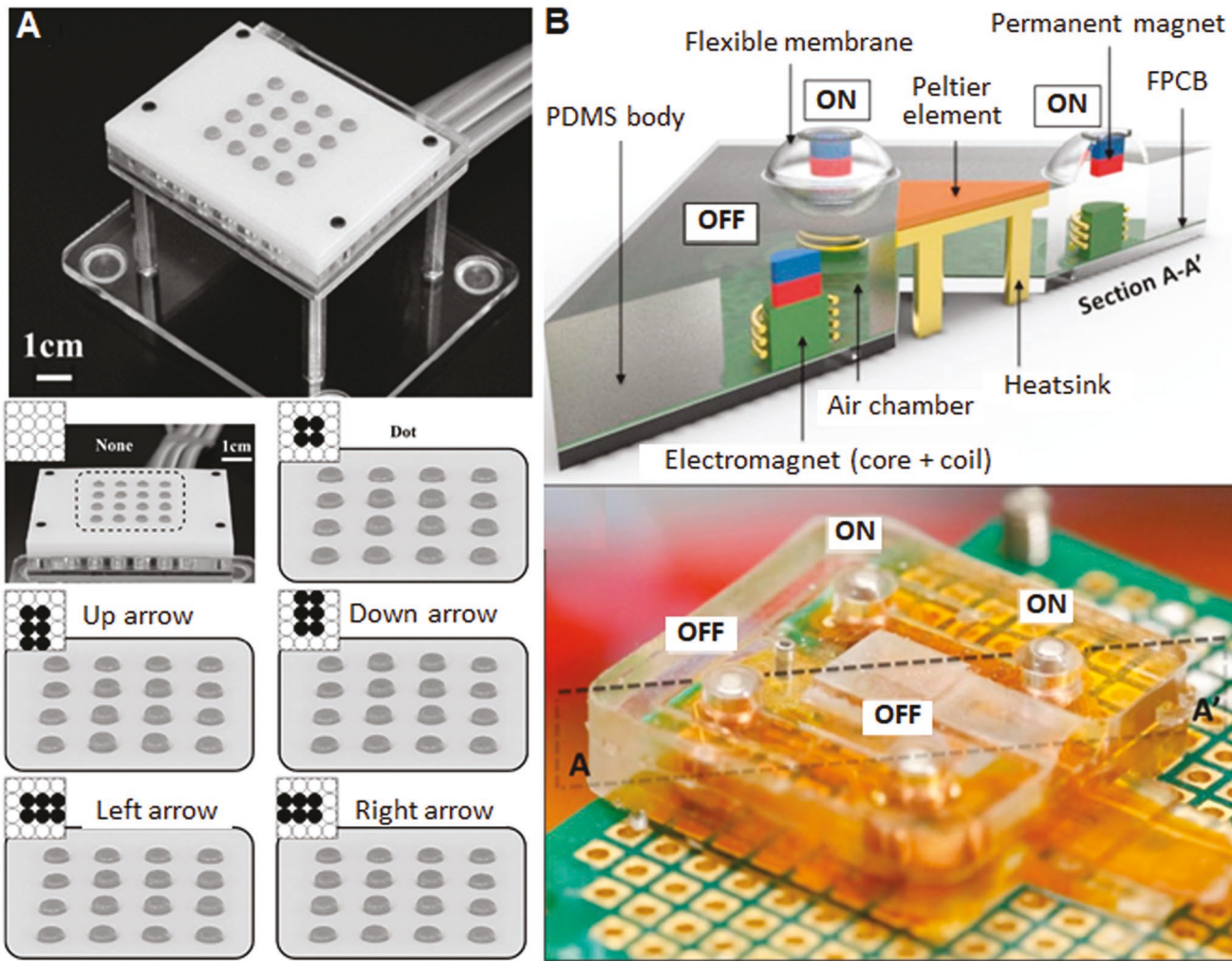


**Figure 10.** Electromagnetic tactile displays. A) Photograph of a tactile display based on electromagnetic actuation showing 4 × 4 taxel haptic display (top) in a 3D printed interface. Images of the tactile display showing six different actuation states presenting six different symbols. Reproduced with permission.<sup>[145]</sup> Copyright 2016, IEEE. B) Schematic device design showing different parts of a single taxel. An image of a final tactile device showing actuation of each cell individually (bottom). Reproduced with permission.<sup>[212]</sup> Copyright 2015, Elsevier B.V.

principles described in the foregoing, in practice, realizing a functional device requires the composition of multiple materials and functionalities. This increases the complexity of the processes used to create the device, and of the device itself, but is essential for practical applications. As one example, Hatada et al. realized a "Haptoskin," which comprised a flexible sheet type tactile display.<sup>[54]</sup> The group used CNTs as electrodes, which were sandwiched in between two PDMS insulators to generate electrostatic vibrations. A MEMS-compatible fabrication process was used to realize the device. Since the CNT and PDMS are flexible and transparent, the final tactile display demonstrated high flexibility and transparency.

#### 6.6.1. Composite Refreshable Braille Displays

Realizing a refreshable Braille display is technologically demanding, but the requirements, expressed in terms of

spatial or temporal resolution, are less severe by 2–3 orders of magnitude. For this reason, they provide a valuable benchmark, and an application that can be of great assistance to those in need. Kato et al. realized a flexible Braille display based on IPMC with integrated transistor.<sup>[133]</sup> Figure 11A shows the schematic cross-section of the device presenting multilayer materials stack in the device (top). The display consisted of a transistor part and an actuator part. The authors used 300  $\mu\text{m}$  thick Nafion as base polymer which was immersed inside dichloro-phenanthroline-gold (III)-chloride complex ( $[\text{AuCl}_2(\text{phen})\text{Cl}]$ ) solution overnight for impregnating Au ions into the Nafion membrane. The membrane was then coated with an electroless plating inside a sodium sulfite solution repeatedly to increase the capacitance of the membrane. Finally the actuators were immersed inside a lithium chloride solution to increase the speed, displacement, and force by exchanging protons with lithium ions. When a voltage is applied to the membrane it deflects rising up a PDMS membrane placed on top of the Nafion film. The

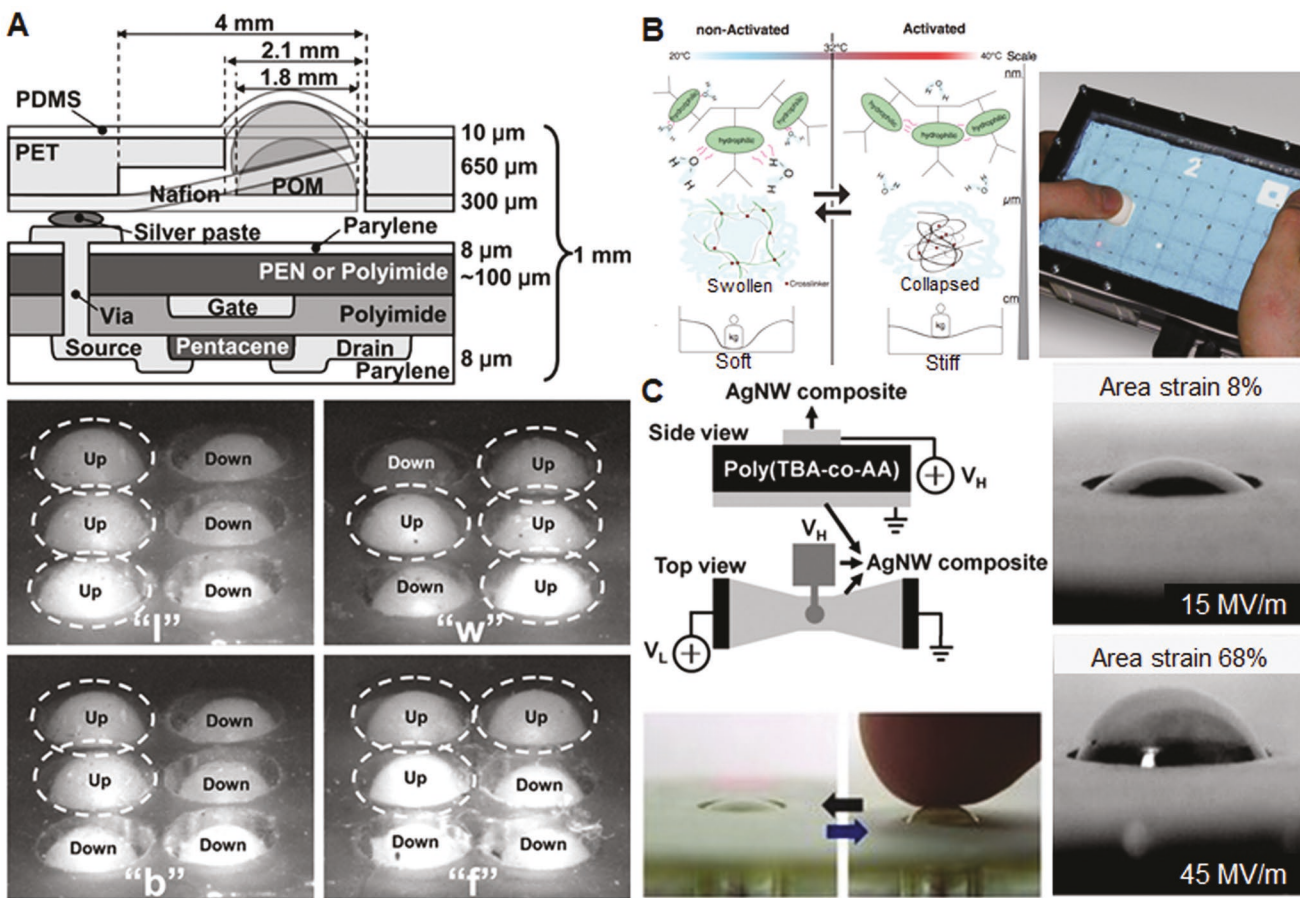


**Figure 11.** Tactile displays based on composite materials. A) Demonstration of a sheet-type Braille display. Schematic design of a single Braille dot based on heterogeneous materials approach showing different device layers and materials (top). Photographs of the Braille sheet display showing several English letters, by actuating individual Braille dots (bottom). Reproduced with permission.<sup>[133]</sup> Copyright 2007, IEEE. B) Schematic presentation of activation mechanisms of PNIPAM polymer through thermal excitation (left) and a photograph of a GelTouch tactile display attached to a touch screen (right). Reproduced with permission.<sup>[63]</sup> Copyright 2015, the authors, published by ACM. C) Ag nanowire based stretchable tactile display. Schematic illustration of the bistable electroactive polymer based stretchable tactile display (top) and photographs of the BSEP based tactile display, a Braille dot under test (bottom). Each Braille dot could respond to different areal strain (right) based on the applied electric field. Reproduced with permission.<sup>[52]</sup> Copyright 2012, WILEY-VCH Verlag GmbH and Co. KGaA, Weinheim.

actuators could show a displacement of 0.4 mm with a force of 1.5 gf at 2.5 V applied voltage. The group realized a  $12 \times 12$  rectangular actuators array. The bottom photographs show the operation of the tactile display. Each Braille dot could be addressed individually via the device-integrated transistor. The English letters "l," "w," "b," and "f" were reproduced as examples. A similar system was described by Okuzaki et al., who realized a tactile display based on a linear actuator that they developed using humido-sensitive conductive polymer.<sup>[242]</sup> They used PEDOT/PSS with various concentrations of poly(4-styrenesulfonate) as the conductive polymer. When 10 V DC bias was applied to a 50 mm long, 2 mm wide, and 16 μm thick PEDOT/PSS film, the film contracted significantly due to the desorption of water vapor in the film since passing current produces Joule heating. The authors used this film to realize a linear actuator by which they realized a tactile display. The actuated Braille cell could display Japanese Braille characters.

#### 6.6.2. Thermoresponsive Gels

Thermoresponsive gels are polymer materials whose mechanical state is altered through the application of heat. They are also interesting for tactile application since they are soft, flexible, and can be transparent. Miruchna et al. developed a system they called GelTouch using a programmable gel.<sup>[63]</sup> The composite gel was realized using polymeric poly(*N*-isopropylacrylamide)-based network (PNIPAM), which is thermoresponsive. This hydrogel changed viscoelasticity and transformed soft to stiff by swallowing water due to thermal excitation. Figure 11B (left) schematically presents the mechanisms of the PNIPAM, the nonactive soft hydrogel becomes stiff when thermally activated. This activation of the polymer also results in an expansion or contraction based on their activation. The group realized a functional prototype based on this polymer (Figure 11B, right). They used an engraved ITO layer with a  $6 \times 4$  array of electrodes that could address each element of the display individually.

### 6.6.3. Multiactuated Systems

In many cases, multiple methods of actuation are combined in order to create highly functional displays. Yun et al. realized a stretchable tactile display using a bistable electroactive polymer (BSEP) and Joule heating.<sup>[52]</sup> The material they developed combined shape memory and dielectric polymers functionalities. The BSEP was developed using shape-memory polyurethane block copolymer (PU) mixing with multiwalled carbon nanotubes (MWNTs), polypyrrole (PPy), and PPy-coated MWNTs. Additionally, for stretchable electrodes, they used silver nanowire–polymer composite with a low sheet resistance. The electrodes could sustain 140% strain without degrading in conductivity. Figure 11C (top) shows a schematic illustration of the tactile display based on BSEP and AgNWs composite. When an electric field was applied to the composite electrodes, it generated Joule heating which deformed the BSEP. The photographs of the tactile display under operation while touched by a finger (bottom) are presented in Figure 11C. The BSEP could achieve different areal strain while applying different electric field to the AgNW composite electrodes that led to different Joule heating (Figure 11C, right).

A similar approach was used by Qiu et al. who realized a high resolution pneumatic tactile display based on BSEP and serpentine-patterned carbon nanotubes.<sup>[72]</sup> The device consisted of a pneumatic part and a BSEP part, and comprised 4 × 4 taxels. The authors reported that the device could exert large stroke and could provide high blocking force. At the same time the device could operate at a low voltage supply with a fast response.

### 6.7. Summary: Advanced Material Technologies for Haptics

The foregoing discussion on haptic devices related to advanced materials clearly indicates that the field has been growing rapidly and numerous functional devices have been demonstrated. The mechanical properties of these devices are also highly important, since haptic devices or tactile displays directly interact with human skin or finger. Engineers have demonstrated a number of wearable tactile displays based on both rigid electronics and flexible electronics. This article has described many of the devices that have been created to date, in this highly active area of research.

Stretchability is also another mechanical phenomenon of electronic devices that has attracted attention for some particular applications. In principle, to make a conformal contact to the body only flexibility is not sufficient, this also requires at least some level of stretchability. There are two ways to realize stretchable system. The first approach uses conventional nonstretchable rigid components as active materials and make the interconnections stretchable, whereas second type uses intrinsically stretchable components and interconnects. However, both types require stretchable substrate. Although most of the reported examples of the stretchable haptic devices are related to sensing<sup>[49,251,252]</sup> and robotic,<sup>[253,254]</sup> there are a few examples of stretchable tactile displays<sup>[50,52,72,99]</sup> based on stretchable

**Table 4.** Selected tactile display technologies based on emerging materials and methods.

Materials	Fabrication methods	Reference
Pneumatic actuators		
PDMS	Microfabrication	[206,207]
PDMS	Micromachining, molding	[73,243]
PDMS, polyurethane	Molding	[209,210]
PDMS, SMP	Casting, 3D printing	[219]
PDMS, acrylic	Molding	[244]
CNT, BSP, urethane diacrylate	Microprocessing	[72]
DEA, hydrogel, silicone	Microprocessing and casting	[245]
Electroactive polymer actuators		
Silicone tube	Micromachining	[246]
Hydrogels, PDMS	Microfabrication, molding	[102,133]
Ionic conducting polymer gel	Mechanical	[247]
PDMS, conductive hydrogel, Ag NWs, PEDOT:PSS	Microprocessing and molding	[51]
Graphene, dielectric elastomer	Microprocessing	[50]
Cellulose, conductive ink	Screen printing	[53]
PET, conductive ink	Inkjet printing	[225]
P(VDF-TrFE-CTFE), elastomer	Transfer printing	[227]
Electrostatic force actuators		
PDMS	Microfabrication	[206,207]
PDMS, metal coil	Molding	[137]
PDMS, graphite	Microprocessing	[98]
PDMS, ITO	Microprocessing and molding	[213,214]
Si, silicone	Microfabrication and micromachining	[248]
Dielectric elastomer	Molding and microprocessing	[99,249]
Elastomer, carbon powder	Molding	[215]
PDMS, CNT	Microfabrication	[54]
Electromagnetic actuators		
PDMS	Microfabrication	[206,207]
PDMS, gold membrane	Molding and microfabrication	[208,216]
PDMS, magnet	Molding and microfabrication	[211,212]
Si, polymer	Microfabrication	[136]
Cellulose electroactive paper	Silk screening	[53]
Fluidic actuators		
Dilatant fluid	Mechanical	[250]
MRF, poly- $\alpha$ -olefin	Mechanical and molding	[59]
MRF, PU foam	Dip coating	[60]
Liquid crystal elastomeric actuators		
LCE, CNTs	Molding and mechanical	[61,62]
Gel actuators		
Hydrogel	Micromachining	[63,64]

actuators. Some of these devices have been discussed earlier and Table 4 presents a short literature review on haptic devices, their mechanisms, and methods used to realize the devices.

## 7. Advanced Materials Technologies: Toward a Tactile Revolution

Analog and digital electronic advances of the past century quickly sparked excitement for the possibility of realizing electronic displays that could reproduce the appearance of familiar objects, people, scenes, and experiences, through video, sound, and even touch. Audiovisual displays—from TV to VR headsets—have found applications far beyond any that were envisaged at the time they were created, greatly impacting education, industry, and culture. The possibility of realizing similar displays for the sense of touch has also attracted considerable attention. However, such devices have steadfastly remained beyond the state-of-the-art.

One reason for this can be traced to the extraordinary human capacities for perceiving objects, surfaces, and scenes via the sense of touch, which rival those of the visual and auditory systems. Touch sensing relies on mechanical signals that span an exceptionally large range of length- and time-scales, including forces and displacements that vary at sub-micrometer length scales and millisecond time scales. Existing technologies short of being able to reproduce such sensations by several orders of magnitude.

A second reason that perceptually accurate tactile displays have eluded realization is that it has proved impractical, in cost and complexity, to realize devices capable of simulating distributed, high-resolution, high-speed, and high dynamic range mechanical signals via conventional micromechanical systems. An interesting comparison can be made to the history of computers. Precomputing inventions, including those of Pascale, Jacquard, and Babbage, were mechanical. These proved impossible to scale to general-purpose computing tasks. Dozens of advances in electronic technologies for computing—proceeding in stages through electromechanical relays, vacuum tubes, transistors, and integrated circuits—were required before modern computers could be built. Eventually, these innovations allowed powerful computers to be integrated into compact devices smaller than a wristwatch. Analogous breakthroughs will be needed in order to realize general purpose tactile displays, but the needed developments are fundamentally different from those that enabled the computing revolution. Realizing such displays will require new material technologies that can bridge the electronic and mechanical domains at the smallest scales.

Today, the path forward is being led by advancements in materials science and engineering, and in methods for designing and fabricating these materials into functional devices and systems. Among the promising developments are those in functional organic materials (whose intrinsic properties of flexibility, stretchability, transparency, and self-healing, which can mirror those of natural biological tissues), emerging nanomaterials with surprising electronic properties, and new methods for multimaterial and multiscale fabrication. This article has reviewed an array of emerging material technologies for haptic feedback. Some of these could one day comprise important milestones in the development of commodity tactile display devices.

Despite considerable research effort, no current technologies can match the sensory capabilities of the tactile skin. To

ameliorate this situation will require advances in several key areas, including the three that we highlight here. The first is to achieve large surface area distributed actuation with fine resolution, high speed, and large amplitudes (or, together, large curvature variations). To achieve this will require highly responsive, elastic functional composites that can achieve high forces within application constraints, such as moderate voltages. This points to a second major challenge, which is to improve the actuation power density (and thus achievable range of forces and bandwidths) of functional materials. For example, one promising family of actuators comprises electrostatic polymer composites. To improve the performance and applicability of these devices will require fundamental advances in organic electronics, including high- $k$  dielectric materials, high dielectric strength insulators, and highly conductive compliant electrodes. Third, we point to the need for new multimaterial, multiscale design and fabrication methods, including automated tools and systems for the design and fabrication of complex multimaterial devices for mass manufacturing. Some of these methods may parallel techniques that have been developed for conventional devices and integrated circuits, while others may leverage unique possibilities for manufacturing new materials, such as multiphoton lithography and roll-to-roll manufacturing of organic electronics.

While the challenges are considerable, the very active nature of research in these areas suggests that the currently large gap between display requirements and the state-of-the-art will continue to shrink. This may lead to future tactile displays that will attain widespread applications, with commensurately large implications for human society and economy.

## Acknowledgements

The authors acknowledge support from the National Science Foundation (NSF-1628831, NSF-1623459, and NSF-1751348). This article is part of the special series on Advanced Intelligent Systems that showcases the outstanding achievements of leading international researchers on intelligent systems.

## Conflict of Interest

The authors declare no conflict of interest.

## Keywords

actuators, haptics, haptic devices, materials, polymers, tactile displays

Received: January 15, 2019

Revised: February 15, 2019

Published online:

- [1] S. Standring, *Gray's Anatomy E-Book: The Anatomical Basis of Clinical Practice*, Elsevier Health Sciences, Philadelphia, USA **2015**.
- [2] R. S. Johansson, J. R. Flanagan, *Nat. Rev. Neurosci.* **2009**, *10*, 345.
- [3] L. Skedung, M. Arvidsson, J. Y. Chung, C. M. Stafford, B. Berglund, M. W. Rutland, *Sci. Rep.* **2013**, *3*, 2617.
- [4] J. M. Loomis, S. J. Lederman, *Handb. Percept. Hum. Perform.* **1986**, *2*, 2.

[5] R. H. LaMotte, M. A. Srinivasan, in *Information Processing in the Somatosensory System*, Macmillan Academic and Professional Ltd., Basingstoke, Hampshire **1991**, pp. 49–58.

[6] Y. Visell, A. Law, J. R. Cooperstock, *IEEE Trans. Haptics* **2009**, 2, 148.

[7] E. R. Kandel, J. H. Schwartz, T. M. Jessell, *Principles of Neural Science*, Vol. 4, McGraw-hill, New York **2000**.

[8] R. L. Klatzky, S. J. Lederman, C. Reed, *J. Exp. Psychol.* **1987**, 116, 356.

[9] C. M. Jones, R. Gray, C. Spence, H. Z. Tan, *Exp. Brain Res.* **2008**, 186, 659.

[10] H. Joodaki, M. B. Panzer, *Proc. Inst. Mech. Eng., Part H* **2018**, 232, 323.

[11] D. Bader, P. Bowker, *Biomaterials* **1983**, 4, 305.

[12] G. Boyer, L. Laquieze, A. Le Bot, S. Laquieze, H. Zahouani, *Skin Res. Technol.* **2009**, 15, 55.

[13] C. Jacquemoud, K. Bruyere-Garnier, M. Coret, *J. Biomech.* **2007**, 40, 468.

[14] M. Geerligs, L. Van Breemen, G. Peters, P. Ackermans, F. Baaijens, C. Oomens, *J. Biomech.* **2011**, 44, 1176.

[15] A. Kalra, A. Lowe, A. Al-Jumaily, *J. Mater. Sci. Eng.* **2016**, 5, 254.

[16] Y. Moayedi, M. Nakatani, E. Lumpkin, in *Scholarpedia of Touch*, Atlantis Press, Paris **2016**, pp. 423–435.

[17] C. F. Bolton, R. Winkelmann, P. J. Dyck, *Neurology* **1966**, 16, 1.

[18] V. B. Mountcastle, *The Sensory Hand: Neural Mechanisms of Somatic Sensation*, Harvard University Press, Cambridge, MA **2005**.

[19] K. O. Johnson, *Curr. Opin. Neurobiol.* **2001**, 11, 455.

[20] Y. Shao, V. Hayward, Y. Visell, *Proc. Natl. Acad. Sci.* **2016**, 113, 4188.

[21] L. A. Jones, A. M. Smith, *Wiley Interdiscip. Rev.: Syst. Biol. Med.* **2014**, 6, 279.

[22] G. A. Gescheider, S. J. Bolanowski, J. V. Pope, R. T. Verrillo, *Somatosens. Mot. Res.* **2002**, 19, 114.

[23] S. J. Bolanowski Jr., G. A. Gescheider, R. T. Verrillo, C. M. Checkosky, *J. Acoust. Soc. Am.* **1988**, 84, 1680.

[24] F. McGlone, D. Reilly, *Neurosci. Biobehav. Rev.* **2010**, 34, 148.

[25] A. B. Vallbo, R. S. Johansson, *Hum. Neurobiol.* **1984**, 3, 3.

[26] R. Johansson, Å. Vallbo, G. Westling, *Brain Res.* **1980**, 184, 343.

[27] R. S. Johansson, R. H. LaMotte, *Somatosens. Res.* **1983**, 1, 21.

[28] H. P. Saal, S. J. Bensmaia, *Neuropsychologia* **2015**, 79, 344.

[29] S. J. Bensmaia, M. Hollins, *J. Acoust. Soc. Am.* **2000**, 108, 1236.

[30] S. J. Lederman, J. M. Loomis, D. A. Williams, *Percept. Psychophys.* **1982**, 32, 109.

[31] M. Cruz, K.-U. Kyung, H. Shea, H. Böse, I. Graz, *IEEE Trans. Haptics* **2018**, 11, 2.

[32] D. Chen, Q. Pei, *Chem. Rev.* **2017**, 117, 11239.

[33] M. O. Martinez, T. K. Morimoto, A. T. Taylor, A. C. Barron, J. A. Pultorak, J. Wang, A. Calasanz-Kaiser, R. L. Davis, P. Blikstein, A. M. Okamura, in *2016 IEEE Haptics Symposium (HAPTICS)*, IEEE, Philadelphia, PA, USA **2016**, pp. 126–133.

[34] D. Escobar-Castillejos, J. Noguez, L. Neri, A. Magana, B. Benes, *J. Med. Syst.* **2016**, 40, 104.

[35] G. Agarwal, N. Besuchet, B. Audergon, J. Paik, *Sci. Rep.* **2016**, 6, 34224.

[36] A. Miriyev, K. Stack, H. Lipson, *Nat. Commun.* **2017**, 8, 596.

[37] R. L. Truby, J. A. Lewis, *Nature* **2016**, 540, 371.

[38] M. Rogóz, H. Zeng, C. Xuan, D. S. Wiersma, P. Wasylczyk, *Adv. Opt. Mater.* **2016**, 4, 1689.

[39] C. Delaney, P. McCluskey, S. Coleman, J. Whyte, N. Kent, D. Diamond, *Lab Chip* **2017**, 17, 2013.

[40] A. M. Nasab, A. Sabzezar, M. Tatari, C. Majidi, W. Shan, *Soft Rob.* **2017**, 4, 411.

[41] P. Polygerinos, Z. Wang, K. C. Galloway, R. J. Wood, C. J. Walsh, *Rob. Auton. Syst.* **2015**, 73, 135.

[42] R. Guo, L. Sheng, H. Gong, J. Liu, *Sci. China: Technol. Sci.* **2018**, 61, 516.

[43] H. Phung, P. T. Hoang, C. T. Nguyen, T. D. Nguyen, H. Jung, U. Kim, H. R. Choi, in *2017 IEEE/RSJ Int. Conf. on Intelligent Robots and Systems (IROS)*, IEEE, Vancouver, BC, Canada **2017**, pp. 886–891.

[44] D. Deepak, M. Ameen, R. Jagan, K. Kumar, *Indian J. Sci. Technol.* **2016**, 9, 42.

[45] K. Shimada, N. Saga, *Sensors* **2016**, 16, 1521.

[46] T. Manouras, M. Vamvakaki, *Polym. Chem.* **2017**, 8, 74.

[47] M. Farajollahi, V. Woehling, C. Plesse, G. T. Nguyen, F. Vidal, F. Sassani, V. X. Yang, J. D. Madden, *Sens. Actuators, A* **2016**, 249, 45.

[48] Y. Bahramzadeh, M. Shahinpoor, *Soft Rob.* **2014**, 1, 38.

[49] K. Jun, J. Kim, I. Oh, *Proc. SPIE* **2018**, 10594, 1059420.

[50] U. Kim, J. Kang, C. Lee, H. Y. Kwon, S. Hwang, H. Moon, J. C. Koo, J.-D. Nam, B. H. Hong, J.-B. Choi, H. R. Choi, *Nanotechnology* **2013**, 24, 145501.

[51] N. Tiwari, M. Rajput, N. A. Chien, N. Mathews, *Small* **2018**, 14, 1702312.

[52] S. Yun, X. Niu, Z. Yu, W. Hu, P. Brochu, Q. Pei, *Adv. Mater.* **2012**, 24, 1321.

[53] G.-Y. Yun, J. Kim, J.-H. Kim, S.-Y. Kim, *Sens. Actuators, A* **2010**, 164, 68.

[54] R. Hatada, H. Ishizuka, M. Kawazoe, N. Miki, in *2016 IEEE 29th Int. Conf. on Micro Electro Mechanical Systems (MEMS)*, IEEE, Shanghai, China **2016**, pp. 1145–1148.

[55] E. Pellicer, J. Sort, *Nanomaterials* **2016**, 6, 15.

[56] A. Alfaedhel, J. Kosel, *Adv. Mater.* **2015**, 27, 7888.

[57] Y. D. Liu, B. M. Lee, T.-S. Park, J. E. Kim, H. J. Choi, S. W. Booh, *J. Colloid Interface Sci.* **2013**, 404, 56.

[58] N.-K. Persson, J. G. Martinez, Y. Zhong, A. Maziz, E. W. Jager, *Adv. Mater. Technol.* **2018**, 3, 1700397.

[59] H. Ishizuka, N. Miki, *Jpn. J. Appl. Phys.* **2017**, 56, 6S1 06GN19.

[60] S. Kim, P. Kim, C.-Y. Park, S.-B. Choi, *Sens. Actuators, A* **2016**, 239, 61.

[61] C. Camargo, H. Campanella, J. Marshall, N. Torras, K. Zinoviev, E. Terentjev, J. Esteve, *J. Micromech. Microeng.* **2012**, 22, 075009.

[62] N. Torras, K. E. Zinoviev, C. J. Camargo, E. M. Campo, H. Campanella, J. Esteve, J. E. Marshall, E. M. Terentjev, M. Omastová, I. Krupa, P. Teplický, B. Mamokka, P. Bruns, B. Roeder, M. Vallribera, R. Malet, S. Zuffanelli, V. Soler, J. Roig, N. Walker, D. Wenn, F. Vossen, F. M. H. Crompvoets, *Sens. Actuators, A* **2014**, 208, 104.

[63] V. Miruchna, R. Walter, D. Lindlbauer, M. Lehmann, R. Von Klitzing, J. Müller, in *Proc. of the 28th Annual ACM Symp. on User Interface Software and Technology*, ACM, Charlotte, NC, USA **2015**, pp. 3–10.

[64] G. Bubak, A. Ansaldo, L. Ceseracciu, K. Hata, D. Ricci, *Proc. SPIE* **2014**, 9056, 905611.

[65] S. J. Biggs, M. A. Srinivasan, *Handbook of Virtual Environments: Design, Implementation, and Applications*, Lawrence Erlbaum Associates, Inc., Mahwah, New Jersey **2002**, pp. 93–116.

[66] F. Connolly, C. J. Walsh, K. Bertoldi, *Proc. Natl. Acad. Sci.* **2017**, 114, 51.

[67] S. Li, D. M. Vogt, D. Rus, R. J. Wood, *Proc. Natl. Acad. Sci.* **2017**, 114, 13132.

[68] J. T. Overvelde, T. Kloek, J. J. Dhaen, K. Bertoldi, *Proc. Natl. Acad. Sci.* **2015**, 112, 10863.

[69] M. Raitor, J. M. Walker, A. M. Okamura, H. Culbertson, in *2017 IEEE Int. Conf. on Robotics and Automation (ICRA)*, IEEE, Singapore, Singapore **2017**, pp. 427–432.

[70] A. Russomanno, Z. Xu, S. O'Modhrain, B. Gillespie, in *2017 IEEE World Haptics Conference (WHC)*, IEEE, Munich, Germany **2017**, pp. 641–646.

[71] R. K. Katschmann, A. de Maille, D. L. Dorhout, D. Rus, in *2016 IEEE/RSJ Int. Conf. on Intelligent Robots and Systems (IROS)*, IEEE, Daejeon, South Korea **2016**, pp. 3048–3055.

[72] Y. Qiu, Z. Lu, Q. Pei, *ACS Appl. Mater. Interfaces* **2018**, *10*, 24807.

[73] C.-H. King, M. Franco, M. O. Culjat, A. T. Higa, J. W. Bisley, E. Dutson, W. S. Grundfest, *J. Med. Devices* **2008**, *2*, 041006.

[74] H. A. Sonar, J. Paik, *Front. Rob. Artif. Intell.* **2016**, *2*, 38.

[75] E. H. Skorina, M. Luo, C. D. Onal, *Front. Rob. Artif. Intell.* **2018**, *5*, 83.

[76] A. A. Stanley, A. M. Okamura, *IEEE Trans. Haptics* **2015**, *8*, 20.

[77] N. Agharese, T. Cloyd, L. H. Blumenschein, M. Raitor, E. W. Hawkes, H. Culbertson, A. M. Okamura, in *2018 IEEE Int. Conf. on Robotics and Automation (ICRA)*, IEEE, Brisbane, QLD, Australia **2018**, pp. 1–5.

[78] A. Russomanno, R. B. Gillespie, S. O’Modhrain, M. Burns, in *2015 IEEE World Haptics Conference (WHC)*, IEEE, Evanston, IL, USA **2015**, pp. 177–182.

[79] K. C. Galloway, K. P. Becker, B. Phillips, J. Kirby, S. Licht, D. Tchernov, R. J. Wood, D. F. Gruber, *Soft Rob.* **2016**, *3*, 23.

[80] Y. Hao, Z. Gong, Z. Xie, S. Guan, X. Yang, Z. Ren, T. Wang, L. Wen, in *2016 35th Chinese Control Conference (CCC)*, IEEE, Chengdu, China **2016**, pp. 6109–6114.

[81] L. Hines, K. Petersen, G. Z. Lum, M. Sitti, *Adv. Mater.* **2017**, *29*, 1603483.

[82] R. V. Martinez, G. M. Whitesides, US Patent 9,797,415, **2017**.

[83] K. H. Petersen, R. F. Shepherd, in *Robotic Systems and Autonomous Platforms*, Woodhead Publishing, Duxford, UK **2019**, pp. 61–84.

[84] C. King, A. T. Higa, M. O. Culjat, S. H. Han, J. W. Bisley, G. P. Carman, E. Dutson, W. S. Grundfest, *Stud. Health Technol. Inf.* **2006**, *125*, 217.

[85] A. D. Marchese, R. K. Katschmann, D. Rus, *Soft Rob.* **2015**, *2*, 7.

[86] E. Acome, S. Mitchell, T. Morrissey, M. Emmett, C. Benjamin, M. King, M. Radakovitz, C. Keplinger, *Science* **2018**, *359*, 61.

[87] D. Ryu, K.-W. Moon, H. Nam, Y. Lee, C. Chun, S. Kang, J.-B. Song, in *IROS 2008, IEEE/RSJ Int. Conf. on Intelligent Robots and Systems, 2008*, IEEE, Nice, France **2008**, pp. 3028–3033.

[88] C. Li, D. Y. Lee, in *2018 18th Int. Conf. on Control, Automation and Systems (ICCAS)*, IEEE, Daegwallyeong, South Korea **2018**, pp. 24–28.

[89] V. Banthia, K. Zareinia, S. Balakrishnan, N. Sepehri, *J. Dyn. Syst., Meas., Control* **2017**, *139*, 111001.

[90] R. W. Johnstone, M. Parameswaran, *Electrostatic Actuators*, Springer US, Boston, MA **2004**, pp. 135–152.

[91] J. M. Schuster, Ph.D. Thesis, Miami University **2018**.

[92] P. Ariano, D. Accardo, M. Lombardi, S. Bocchini, L. Draghi, L. De Nardo, P. Fino, *J. Appl. Biomater. Funct. Mater.* **2015**, *13*, 1.

[93] R. E. Pelrine, R. D. Kornbluh, J. P. Joseph, *Sens. Actuators, A* **1998**, *64*, 77.

[94] R. Pelrine, R. Kornbluh, Q. Pei, J. Joseph, *Science* **2000**, *287*, 836.

[95] C. Keplinger, T. Li, R. Baumgartner, Z. Suo, S. Bauer, *Soft Matter* **2012**, *8*, 285.

[96] W.-H. Park, J. W. Bae, E.-J. Shin, S.-Y. Kim, *Smart Mater. Struct.* **2016**, *25*, 115020.

[97] W.-H. Park, E.-J. Shin, S. Yun, S.-Y. Kim, *IEEE Trans. Haptics* **2018**, *11*, 22.

[98] M. Matysek, P. Lotz, T. Winterstein, H. F. Schlaak, in *Third Joint EuroHaptics Conf., 2009 and Symp. on Haptic Interfaces for Virtual Environment and Teleoperator Systems, World Haptics 2009*, IEEE, Salt Lake City, UT, USA **2009**, pp. 290–295.

[99] H. S. Lee, H. Phung, D.-H. Lee, U. K. Kim, C. T. Nguyen, H. Moon, J. C. Koo, J.-D. Nam, H. R. Choi, *Sens. Actuators, A* **2014**, *205*, 191.

[100] S. Rosset, H. R. Shea, *Appl. Phys. Rev.* **2016**, *3*, 031105.

[101] Y. Bar-Cohen, *Electroactive Polymer (EAP) Actuators as Artificial Muscles: Reality, Potential, and Challenges*, Vol. 5, SPIE Press, Bellingham, WA **2004**.

[102] G. Paschew, A. Richter, *Proc. SPIE* **2010**, *7642*, 764234.

[103] C. D. Shultz, M. A. Peshkin, J. E. Colgate, in *2015 IEEE World Haptics Conference (WHC)*, IEEE, Evanston, IL, USA **2015**, pp. 57–62.

[104] C. Shultz, E. Colgate, M. A. Peshkin, *IEEE Trans. Haptics* **2018**, *11*, 279.

[105] K. A. Kaczmarek, K. Nammi, A. K. Agarwal, M. E. Tyler, S. J. Haase, D. J. Beebe, *IEEE Trans. Biomed. Eng.* **2006**, *53*, 2047.

[106] O. Bau, I. Poupyrev, A. Israr, C. Harrison, in *Proc. of the 23rd Annual ACM Symp. on User Interface Software and Technology*, ACM, New York, NY, USA **2010**, pp. 283–292.

[107] J. Kang, H. Kim, S. Choi, K.-D. Kim, J. Ryu, *IEEE Trans. Haptics* **2017**, *10*, 371.

[108] Y. Vardar, B. Güçlü, C. Basdogan, *IEEE Trans. Haptics* **2017**, *10*, 488.

[109] S. Kapoor, P. Arora, V. Kapoor, M. Jayachandran, M. Tiwari, *J. Clin. Diagn. Res.* **2014**, *8*, 294.

[110] H. Ishizuka, R. Hatada, C. Cortes, N. Miki, *Micromachines* **2018**, *9*, 230.

[111] T. Ninomiya, Y. Okayama, Y. Matsumoto, X. Arouette, K. Osawa, N. Miki, *Sens. Actuators, A* **2011**, *166*, 277.

[112] R. Atkinson, *J. Phys. D: Appl. Phys.* **1969**, *2*, 325.

[113] J. Mullenbach, M. Peshkin, J. E. Colgate, in *2016 IEEE Haptics Symposium (HAPTICS)*, IEEE, Philadelphia, PA, USA **2016**, pp. 271–276.

[114] S. S. Rao, M. Sunar, *Appl. Mech. Rev.* **1994**, *47*, 113.

[115] J. G. Smits, S. I. Dalke, T. K. Cooney, *Sens. Actuators, A* **1991**, *28*, 41.

[116] B. Hannaford, A. M. Okamura, in *Springer Handbook of Robotics*, Springer, Cham, Switzerland **2016**, pp. 1063–1084.

[117] B. Sauvet, T. Laliberte, C. Gosselin, *Mechatronics* **2017**, *45*, 100.

[118] I.-T. Seo, T.-G. Lee, D.-H. Kim, J. Hur, J.-H. Kim, S. Nahm, J. Ryu, B.-Y. Choi, *Sens. Actuators, A* **2016**, *238*, 71.

[119] T. Kodama, S. Izumi, K. Masaki, H. Kawaguchi, K. Maenaka, M. Yoshimoto, in *2015 37th Annual Int. Conf. of the IEEE, Engineering in Medicine and Biology Society (EMBC)*, IEEE, Milan, Italy **2015**, pp. 1172–1175.

[120] P. Laitinen, J. Mawnpaa, in *IEEE Int. Workshop on Haptic Audio Visual Environments and Their Applications, 2006, HAVE 2006*, IEEE, Ottawa, Ont., Canada **2006**, pp. 40–43.

[121] I. Poupyrev, S. Maruyama, J. Rekimoto, in *Proc. of the 15th Annual ACM Symp. on User Interface Software and Technology*, ACM, Paris, France **2002**, pp. 51–60.

[122] K. S. Ramadan, D. Sameoto, S. Evoy, *Smart Mater. Struct.* **2014**, *23*, 033001.

[123] C. Dagdeviren, Y. Shi, P. Joe, R. Ghaffari, G. Balooch, K. Usgaonkar, O. Gur, P. L. Tran, J. R. Crosby, M. Meyer, Y. Su, R. Chad Webb, A. S. Tedesco, M. J. Slepian, Y. Huang, J. A. Rogers, *Nat. Mater.* **2015**, *14*, 728.

[124] Q. Wang, V. Hayward, in *2006 14th Symp. on Haptic Interfaces for Virtual Environment and Teleoperator Systems*, IEEE, Alexandria, VA, USA **2006**, pp. 67–72.

[125] P. Olsson, F. Nysjö, I. B. Carlbom, S. Johansson, *IEEE Trans. Haptics* **2016**, *9*, 427.

[126] A. Akther, A. Kafy, L. Zhai, H. C. Kim, M. I. R. Shishir, J. Kim, *Smart Mater. Struct.* **2016**, *25*, 115043.

[127] D. G. Seo, Y.-H. Cho, *J. Mech. Sci. Technol.* **2018**, *32*, 631.

[128] L. Chang, L. Yu, C. Li, Q. Niu, Y. Hu, P. Lu, Z. Zhu, Y. Wu, *Smart Mater. Struct.* **2018**, *27*, 105046.

[129] C. Jo, D. Pugal, I.-K. Oh, K. J. Kim, K. Asaka, *Prog. Polym. Sci.* **2013**, *38*, 1037.

[130] K. Kruusamäe, A. Punning, A. Aabloo, K. Asaka, in *Actuators*, Vol. 4, MDPI AG, Basel, Switzerland **2015**, pp. 17–38.

[131] M. Shahinpoor, *The Royal Society of Chemistry*, Cambridge, UK **2015**, pp. 311–340.

[132] M. Shahinpoor, Y. Bar-Cohen, J. Simpson, J. Smith, *Smart Mater. Struct.* **1998**, 7, 6 R15.

[133] Y. Kato, T. Sekitani, M. Takamiya, M. Doi, K. Asaka, T. Sakurai, T. Someya, *IEEE Trans. Electron Devices* **2007**, 54, 202.

[134] T. A. Nguyen, C.-J. Peng, K. Rohtlaid, C. Plesse, T.-M. G. Nguyen, F. Vidal, S.-J. Chen, L. Chassagne, B. Cagneau, *Sens. Actuators, A* **2018**, 272, 325.

[135] T. N. Nguyen, K. Rohtlaid, C. Plesse, G. T. Nguyen, C. Soyer, S. Grondel, E. Cattan, J. D. Madden, F. Vidal, *Electrochim. Acta* **2018**, 265, 670.

[136] S. Youn, D. G. Seo, Y.-H. Cho, *Sens. Actuators, A* **2013**, 195, 105.

[137] K. Na, J.-S. Han, D.-M. Roh, B.-K. Chae, E.-S. Yoon, J. Y. Kang, I.-J. Cho, in *2012 IEEE 25th Int. Conf. on Micro Electro Mechanical Systems (MEMS)*, IEEE, Paris, France **2012**, pp. 1149–1152.

[138] J. J. Zárate, G. Tosolini, S. Petroni, M. De Vittorio, H. Shea, *Sens. Actuators, A* **2015**, 234, 57.

[139] T. N. Do, H. Phan, T.-Q. Nguyen, Y. Visell, *Adv. Funct. Mater.* **2018**, 28, 1800244.

[140] B. Hanson, M. Levesley, *Sens. Actuators, A* **2004**, 116, 345.

[141] O. Bau, U. Petrevski, W. Mackay, in *CHI'09 Extended Abstracts on Human Factors in Computing Systems*, ACM, Boston, MA, USA **2009**, pp. 3607–3612.

[142] R. Riener, T. Villgrattner, R. Kleiser, T. Nef, S. Kollias, in *27th Annual Int. Conf. of the Engineering in Medicine and Biology Society, 2005, IEEE-EMBS 2005*, IEEE, Shanghai, China **2006**, pp. 7024–7027.

[143] F. Pece, J. J. Zárate, V. Vechev, N. Besse, O. Gudozhnik, H. Shea, O. Hilliges, in *Proc. of the 30th Annual ACM Symp. on User Interface Software and Technology*, ACM, Québec City, QC, Canada **2017**, pp. 143–154.

[144] C. Bolzmacher, G. Chalubert, O. Brelaud, J.-P. Alexander, M. Hafez, in *Int. Conf. on Human Haptic Sensing and Touch Enabled Computer Applications*, Springer, Berlin, Heidelberg **2014**, pp. 333–341.

[145] J. J. Zárate, H. Shea, *IEEE Trans. Haptics* **2017**, 10, 106.

[146] Y. Liu, R. Davidson, P. Taylor, *Proc. SPIE* **2007**, 6423, 642331.

[147] R. Firoozian, in *Servo Motors and Industrial Control Theory*, Springer, Cham, Switzerland **2009**, pp. 119–130.

[148] P. Sheng, W. Wen, *Annu. Rev. Fluid Mech.* **2012**, 44, 143.

[149] Y. Liu, R. Davidson, P. Taylor, *Proc. SPIE* **2005**, 5764, 92.

[150] D. Klein, H. Freimuth, G. Monkman, S. Egersdörfer, A. Meier, H. Böse, M. Baumann, H. Ermert, O. Bruhns, *Mechatronics* **2005**, 15, 883.

[151] Y.-M. Han, P.-S. Kang, K.-G. Sung, S.-B. Choi, *J. Intell. Mater. Syst. Struct.* **2007**, 18, 1149.

[152] J. Melli-Huber, B. Weinberg, A. Fisch, J. Nikitczuk, C. Mavroidis, C. Wampler, in *Proc. of the 11th Symposium on Haptic Interfaces for Virtual Environment and Teleoperator Systems*, 2003, HAPTICS 2003, IEEE, Los Angeles, CA, USA **2003**, pp. 262–269.

[153] C. Mavroidis, Y. Bar-Cohen, M. Bouzit, *Electroactive Polymer Actuators as Artificial Muscles: Reality, Potentials, and Challenges*, SPIE Press, Bellingham, WA **2001**, pp. 567–594.

[154] Y.-H. Hwang, S.-R. Kang, S.-W. Cha, S.-B. Choi, *Sens. Actuators, A* **2016**, 249, 163.

[155] A. J. Mazursky, J.-H. Koo, T.-H. Yang, *Proc. SPIE* **2018**, 10595, 105951M.

[156] G. J. Monkman, in *Presence: Teleoperators and Virtual Environments*, Vol. 1, MIT Press **1992**, p. 219.

[157] Y. Liu, R. Davidson, P. Taylor, *Smart Mater. Struct.* **2005**, 14, 1563.

[158] H. D. Garner, *Method and Device for Producing a Tactile Display Using an Electrorheological Fluid* **1996**, US5496174A.

[159] Y. Jansen, T. Karrer, J. Borchers, in *Adjunct Proc. of the 23rd Annual ACM Symp. on User Interface Software and Technology*, ACM, New York, NY, USA **2010**, pp. 385–386.

[160] N. Takesue, J. Furusho, Y. Kiyota, *JSME Int. J., Ser. C* **2004**, 47, 783.

[161] T. Kikuchi, J. Noma, S. Akaiwa, Y. Ueshima, *J. Intell. Mater. Syst. Struct.* **2016**, 27, 859.

[162] J. D. Carlson, M. R. Jolly, *Mechatronics* **2000**, 10, 555.

[163] M. G. Muriuki, W. W. Clark, *Proc. SPIE* **1999**, 3672, 55.

[164] P. Kim, S. Kim, Y.-D. Park, S.-B. Choi, *Smart Mater. Struct.* **2016**, 25, 035008.

[165] G. Savioz, V. Ruchet, Y. Perriard, in *2010 IEEE/ASME Int. Conf. on Advanced Intelligent Mechatronics (AIM)*, IEEE, Montreal, ON, Canada **2010**, pp. 1197–1202.

[166] S. Ryu, J.-H. Koo, T.-H. Yang, D. Pyo, K.-U. Kyung, D.-S. Kwon, *J. Intell. Mater. Syst. Struct.* **2015**, 26, 1670.

[167] A. Berrezag, Y. Visell, V. Hayward, in *Int. Conf. on Human Haptic Sensing and Touch Enabled Computer Applications*, Springer, Berlin, Heidelberg **2012**, pp. 186–190.

[168] Y. Liu, R. Davidson, P. Taylor, J. Ngu, J. Zarraga, *Displays* **2005**, 26, 29.

[169] R. Rizzo, A. Musolino, L. A. Jones, *IEEE Trans. Haptics* **2018**, 11, 317.

[170] H. Ishizuka, N. Miki, in *2016 IEEE 29th Int. Conf. on Micro Electro Mechanical Systems (MEMS)*, IEEE, Shanghai, China **2016**, pp. 1165–1168.

[171] Y.-M. Han, J.-S. Oh, J.-K. Kim, S.-B. Choi, *Smart Mater. Struct.* **2014**, 23, 077001.

[172] R. S. Kularatne, H. Kim, J. M. Boothby, T. H. Ware, *J. Polym. Sci., Part B: Polym. Phys.* **2017**, 55, 395.

[173] C. Ohm, M. Brehmer, R. Zentel, *Adv. Mater.* **2010**, 22, 3366.

[174] H. Jiang, C. Li, X. Huang, *Nanoscale* **2013**, 5, 5225.

[175] A. Buguin, M.-H. Li, P. Silberzan, B. Ladoux, P. Keller, *J. Am. Chem. Soc.* **2006**, 128, 1088.

[176] Y. Yu, T. Ikeda, *Angew. Chem., Int. Ed.* **2006**, 45, 5416.

[177] L. Yang, K. Setyowati, A. Li, S. Gong, J. Chen, *Adv. Mater.* **2008**, 20, 2271.

[178] T. J. White, D. J. Broer, *Nat. Mater.* **2015**, 14, 1087.

[179] M. Camacho-Lopez, H. Finkelmann, P. Palfy-Muhoray, M. Shelley, *Nat. Mater.* **2004**, 3, 307.

[180] S. Maeda, Y. Hara, R. Yoshida, S. Hashimoto, *Int. J. Mol. Sci.* **2010**, 11, 52.

[181] T. Jayaramudu, Y. Li, H.-U. Ko, I. R. Shishir, J. Kim, *Int. J. Precis. Eng. Manuf.-Green Technol.* **2016**, 3, 375.

[182] A. Khan, Z. Abas, H. Kim, J. Kim, *Sensors* **2016**, 16, 1172.

[183] D. Chen, J. Yoon, D. Chandra, A. J. Crosby, R. C. Hayward, *J. Polym. Sci., Part B: Polym. Phys.* **2014**, 52, 1441.

[184] Y. Zheng, J. Cui, in *Des., Fabr., Prop. Appl. Smart Adv. Mater.*, CRC Press, FL **2016**, p. 275.

[185] S. M. R. Billah, M. I. H. Mondal, S. H. Somoal, M. N. Pervez, *Cellulose-Based Superabsorbent Hydrogels*, Springer International Publishing, Switzerland **2018**, pp. 1–41.

[186] Y. Takashima, Y. Hayashi, M. Osaki, F. Kaneko, H. Yamaguchi, A. Harada, *Macromolecules* **2018**.

[187] M. K. Purkait, M. K. Sinha, P. Mondal, R. Singh, in *Interface Science and Technology*, Vol. 25, Elsevier, London, UK **2018**, pp. 193–219.

[188] D. Morales, E. Palleau, M. D. Dickey, O. D. Velev, *Soft Matter* **2014**, 10, 1337.

[189] A. Kheyreddini Mousavi, S. Alaie, Z. C. Leseman, *Encyclopedia of Nanotechnology*, Springer, Netherlands **2016**, pp. 1–16.

[190] K. Kanda, K. Takahara, S. Toyama, T. Fujita, K. Maenaka, *Jpn. J. Appl. Phys.* **2018**, 57, 11UF14.

[191] H. Ishizuka, N. Miki, *Displays* **2015**, 37, 25.

[192] A. Sieber, P. Valdastri, K. Houston, C. Eder, O. Tonet, A. Menciassi, P. Dario, *Sens. Actuators, A* **2008**, 142, 19.

[193] T. Mineta, H. Yanatori, K. Hiroyoshi, K. Tsuji, Y. Ono, K. Abe, in *2017 19th Int. Conf. on Solid-State Sensors, Actuators and Microsystems (TRANSDUCERS)*, IEEE, Kaohsiung, Taiwan **2017**, pp. 2031–2034.

[194] A. Charalambides, S. Bergbreiter, *J. Micromech. Microeng.* **2015**, *25*, 095009.

[195] A. Charalambides, J. Cheng, T. Li, S. Bergbreiter, in *2015 28th IEEE Int. Conf. on Micro Electro Mechanical Systems (MEMS)*, IEEE, Estoril, Portugal **2015**, pp. 726–729.

[196] A. Nespoli, S. Besseghini, S. Pittaccio, E. Villa, S. Viscuso, *Sens. Actuators, A* **2010**, *158*, 149.

[197] F. Zhao, K. Fukuyama, H. Sawada, in *the 18th IEEE Int. Symp. on Robot and Human Interactive Communication*, 2009, RO-MAN 2009, IEEE, Toyama, Japan **2009**, pp. 28–33.

[198] M. C. Yip, G. Niemeyer, in *2015 IEEE Int. Conf. on Robotics and Automation (ICRA)*, IEEE, Seattle, WA, USA **2015**, pp. 2313–2318.

[199] L. Sutton, H. Moein, A. Rafiee, J. D. Madden, C. Menon, in *2016 6th IEEE Int. Conf. on Biomedical Robotics and Biomechatronics (BioRob)*, IEEE, Singapore, Singapore **2016**, pp. 1074–1079.

[200] M. Shikida, T. Imamura, S. Ukai, T. Miyaji, K. Sato, *J. Micromech. Microeng.* **2008**, *18*, 065012.

[201] S. Kurzhals, R. Zirbs, E. Reimhult, *ACS Appl. Mater. Interfaces* **2015**, *7*, 19342.

[202] H. Cheng, J. Liu, Y. Zhao, C. Hu, Z. Zhang, N. Chen, L. Jiang, L. Qu, *Angew. Chem., Int. Ed.* **2013**, *52*, 10482.

[203] J. Zhou, S. A. Turner, S. M. Brosnan, Q. Li, J.-M. Y. Carrillo, D. Nykypanchuk, O. Gang, V. S. Ashby, A. V. Dobrynin, S. S. Sheiko, *Macromolecules* **2014**, *47*, 1768.

[204] D.-D. Han, Y.-L. Zhang, J.-N. Ma, Y.-Q. Liu, B. Han, H.-B. Sun, *Adv. Mater.* **2016**, *28*, 8328.

[205] X. Zhang, Z. Yu, C. Wang, D. Zarrouk, J.-W. T. Seo, J. C. Cheng, A. D. Buchan, K. Takei, Y. Zhao, J. W. Ager, J. Zhang, M. Hettick, M. C. Hersam, A. P. Pisano, R. S. Fearing, A. Javey, *Nat. Commun.* **2014**, *5*, 2983.

[206] H.-J. Kwon, S. W. Lee, S. S. Lee, *Sens. Actuators, A* **2009**, *154*, 238.

[207] S. R. Green, B. J. Gregory, N. K. Gupta, in *5th IEEE Conf. on Sensors*, 2006, IEEE, Daegu, South Korea **2006**, pp. 307–310.

[208] H. S. Lee, D. H. Lee, D. G. Kim, U. K. Kim, C. H. Lee, N. N. Linh, N. C. Toan, J. C. Koo, H. Moon, J. Nam, J. Han, H. R. Choi, *Proc. SPIE* **2012**, *8340*, 83400E.

[209] X. Wu, S.-H. Kim, H. Zhu, C.-H. Ji, M. G. Allen, *J. Microelectromech. Syst.* **2012**, *21*, 908.

[210] E. Doh, J. Yoo, H. Lee, J. Park, K.-S. Yun, *Jpn. J. Appl. Phys.* **2012**, *52*, 1R 017302.

[211] C. Son, K. Ko, H. J. Lee, K. Na, J. Han, K.-S. Yun, E.-S. Yoon, E. Kim, I.-J. Cho, *Microsyst. Technol.* **2016**, *22*, 2587.

[212] S. Gallo, C. Son, H. J. Lee, H. Bleuler, I.-J. Cho, *Sens. Actuators, A* **2015**, *236*, 180.

[213] D. Pyo, S. Ryu, S.-C. Kim, D.-S. Kwon, in *Int. Conf. on Human Haptic Sensing and Touch Enabled Computer Applications*, Springer, Berlin, Heidelberg **2014**, pp. 487–495.

[214] S.-Y. Kim, K.-b. Kim, J. Kim, K.-u. Kyung, in *Int. Workshop on Haptic and Audio Interaction Design*, Springer, Berlin, Heidelberg **2013**, pp. 109–116.

[215] I. Koo, K. Jung, J. Koo, J. D. Nam, Y. Lee, H. R. Choi, in *Proc. 2006 IEEE Int. Conf. on Robotics and Automation*, 2006, ICRA 2006, IEEE, **2006**, pp. 2220–2225.

[216] J. Streque, A. Talbi, P. Pernod, V. Preobrazhensky, in *Int. Conf. on Human Haptic Sensing and Touch Enabled Computer Applications*, Springer, Berlin, Heidelberg **2008**, pp. 437–446.

[217] H. Bikas, P. Stavropoulos, G. Chryssolouris, *Int. J. Adv. Manuf. Technol.* **2016**, *83*, 389.

[218] Y.-L. Feng, R. L. Peiris, C. L. Fernando, K. Minamizawa, in *Int. Conf. on Human Haptic Sensing and Touch Enabled Computer Applications*, Springer, Cham **2018**, pp. 180–192.

[219] N. Besse, S. Rosset, J. J. Zarate, H. Shea, *Adv. Mater. Technol.* **2017**, *2*, 1700102.

[220] M. P. Chae, F. Lin, R. T. Spychal, D. J. Hunter-Smith, W. M. Rozen, *Microsurgery* **2015**, *35*, 148.

[221] M. Vázquez, E. Brockmeyer, R. Desai, C. Harrison, S. E. Hudson, in *Proc. of the 33rd Annual ACM Conf. on Human Factors in Computing Systems*, ACM, Seoul, Republic of Korea **2015**, pp. 1295–1304.

[222] S. Pyo, J.-I. Lee, M.-O. Kim, T. Chung, Y. Oh, S.-C. Lim, J. Park, J. Kim, *J. Micromech. Microeng.* **2014**, *24*, 075012.

[223] F. Beruscha, W. Krautter, Y. H. So, J. H. Jeon, in *Proc. of the 2018 ACM Int. Joint Conf. and 2018 Int. Symp. on Pervasive and Ubiquitous Computing and Wearable Computers*, ACM, Singapore, Singapore **2018**, pp. 9–12.

[224] D. McCallum, S. Ungar, *An Introduction to the Use of Inkjet for Tactile Diagram Production*, **2003**.

[225] K. Kato, H. Miyashita, H. Kajimoto, H. Ishizuka, in *Adjunct Publication of the 30th Annual ACM Symp. on User Interface Software and Technology*, ACM, Québec City, QC, Canada **2017**, pp. 31–33.

[226] M. A. Price, F. C. SupIV, *IEEE/ASME Trans. Mechatronics* **2018**, *23*, 2347.

[227] W.-E. Ju, Y.-J. Moon, C.-H. Park, S. T. Choi, *Smart Mater. Struct.* **2014**, *23*, 074004.

[228] S. T. Choi, J. O. Kwon, F. Bauer, *Sens. Actuators, A* **2013**, *203*, 282.

[229] S. S. Robinson, K. W. O'Brien, H. Zhao, B. N. Peele, C. M. Larson, B. C. Mac Murray, I. M. Van Meerbeek, S. N. Dunham, R. F. Shepherd, *Extreme Mech. Lett.* **2015**, *5*, 47.

[230] T. Kamigaki, A. Noda, H. Shinoda, in *2017 56th Annual Conf. of the Society of Instrument and Control Engineers of Japan (SICE)*, IEEE, Kanazawa, Japan **2017**, pp. 736–739.

[231] G. Ilkhani, E. Samur, in *2018 IEEE Haptics Symposium (HAPTICS)*, IEEE, San Francisco, CA, USA **2018**, pp. 163–168.

[232] M. Tezuka, N. Kitamura, K. Tanaka, N. Miki, *PLoS One* **2016**, *11*, e0148410.

[233] H. Phung, C. T. Nguyen, T. D. Nguyen, C. Lee, U. Kim, D. Lee, J.-D. Nam, H. Moon, J. C. Koo, H. R. Choi, *Meccanica* **2015**, *50*, 2825.

[234] A. Marette, A. Poulin, N. Besse, S. Rosset, D. Briand, H. Shea, *Adv. Mater.* **2017**, *29*, 1700880.

[235] I. M. Koo, K. Jung, J. C. Koo, J.-D. Nam, Y. K. Lee, H. R. Choi, *IEEE Trans. Rob.* **2008**, *24*, 549.

[236] G. Frediani, D. Mazzei, D. E. De Rossi, F. Carpi, *Front. Bioeng. Biotechnol.* **2014**, *2*, 31.

[237] V. Diener, M. Beigl, M. Budde, E. Pescara, in *Proc. of the 2017 ACM Int. Symp. on Wearable Computers*, ACM, Maui, Hawaii **2017**, pp. 82–89.

[238] R. C. Me, V. Ferraro, A. Biamonti, in *Int. Conf. on Wireless Mobile Communication and Healthcare*, Springer, Cham **2016**, pp. 406–414.

[239] M. Rotard, C. Taras, T. Ertl, *Multimedia Tools Appl.* **2008**, *37*, 53.

[240] J. Streque, A. Talbi, P. Pernod, V. Preobrazhensky, *J. Micromech. Microeng.* **2012**, *22*, 095020.

[241] K. Deng, E. T. Enikov, *Mechatronics* **2010**, *20*, 503.

[242] H. Okuzaki, K. Hosaka, H. Suzuki, T. Ito, *React. Funct. Polym.* **2013**, *73*, 986.

[243] C.-H. King, M. O. Culjat, M. L. Franco, J. W. Bisley, E. Dutson, W. S. Grundfest, *IEEE Trans. Biomed. Eng.* **2008**, *55*, 2593.

[244] L. Santos-Carreras, K. Leuenberger, P. Rétornaz, R. Gassert, H. Bleuler, in *2010 IEEE/RSJ Int. Conf. on Intelligent Robots and Systems (IROS)*, IEEE, Taipei, Taiwan **2010**, pp. 5060–5066.

[245] C. Larson, B. Peele, S. Li, S. Robinson, M. Totaro, L. Beccai, B. Mazzolai, R. Shepherd, *Science* **2016**, *351*, 1071.

[246] P. Chakraborti, H. K. Toprakci, P. Yang, N. Di Spigna, P. Franzon, T. Ghosh, *Sens. Actuators, A* **2012**, *179*, 151.

[247] M. Konyo, S. Tadokoro, T. Takamori, in *Proc. IEEE Int. Conf. on Robotics and Automation*, 2000, ICRA'00, Vol. 4, IEEE, **2000**, pp. 3416–3421.

[248] H. Sasaki, M. Shikida, K. Sato, *J. Micromech. Microeng.* **2006**, *16*, 2673.

[249] H. R. Choi, D. Kim, N. H. Chuc, N. H. L. Vuong, J. Koo, J.-d. Nam, Y. Lee, *Proc. SPIE* **2009**, 7287, 72871C.

[250] S. Saga, K. Deguchi, in *2010 IEEE Haptics Symposium*, IEEE, Waltham, MA, USA **2010**, pp. 309–312.

[251] R. K. Kramer, C. Majidi, R. J. Wood, in *2011 IEEE Int. Conf. on Robotics and Automation (ICRA)*, IEEE, **2011**, pp. 1103–1107.

[252] S. Biswas, J. Reiprich, J. Pezoldt, T. Stauden, H. O. Jacobs, *Adv. Mater. Technol.* **2019**, 1800446.

[253] M.-A. Lacasse, V. Duchaine, C. Gosselin, in *2010 IEEE Int. Conf. on Robotics and Automation (ICRA)*, IEEE, Anchorage, AK, USA **2010**, pp. 4842–4848.

[254] K. Noda, E. Iwase, K. Matsumoto, I. Shimoyama, in *2010 IEEE Int. Conf. on Robotics and Automation (ICRA)*, IEEE, Anchorage, AK, USA **2010**, pp. 4212–4217.